Translational Oncology 43 (2024) 101857

Contents lists available at ScienceDirect

Translational Oncology

journal homepage: www.elsevier.com/locate/tranon

Original Research

The highly selective and oral phosphoinositide 3-kinase delta (PI3K-δ) inhibitor roginolisib induces apoptosis in mesothelioma cells and increases immune effector cell composition

Claudia Kalla [a,b,c], German Ott [b], Francesca Finotello [d], Karolina Niewola-Staszkowska [e], Giusy Di Conza [e], Michael Lahn [e], Lars van der Veen [e], Julia Schüler [f], Roger Falkenstern-Ge [g], Joanna Kopecka [h,i], Chiara Riganti [h,i,j,*]

[a] Dr. Margarete Fischer-Bosch Institute of Clinical Pharmacology, Auerbachstrasse 112, 70376, Stuttgart, Germany
[b] Department of Clinical Pathology, Robert-Bosch-Krankenhaus, Auerbachstrasse 112, 70376, Stuttgart, Germany
[c] Department of Clinical Pharmacology, University Hospital, University of Tuebingen, Auf der Morgenstelle 8, 72076, Tuebingen, Germany
[d] Department of Molecular Biology, Digital Science Center (DiSC), Universität Innsbruck, Innrain 15, A-6020 Innsbruck, Austria
[e] iOnctura SA, Avenue Secheron 15, 1202, Geneva, Switzerland
[f] Charles River Germany GmbH, Am Flughafen 12, Freiburg, Germany
[g] Department of Molecular and Pneumonological Oncology, Robert-Bosch-Krankenhaus, Auerbachstrasse 112, 70376, Stuttgart, Germany
[h] Department of Oncology, University of Torino, via Nizza 44, 10126, Torino, Italy
[i] Molecular Biotechnology Center "Guido Tarone", via Nizza 44, 10126, Torino, Italy
[j] Interdepartmental Center "G.Scansetti" for the study of asbestos and other toxic particulates, University of Torino, 10126 Torino, Italy

ARTICLE INFO

Keywords:
Phosphoinositide 3-kinase delta (PI3K-δ)
malignant pleural mesothelioma
PI3/AKT/mTOR inhibition
apoptosis
tumor induced-immunosuppression
combinatorial therapy

ABSTRACT

Targeting aberrantly expressed kinases in malignant pleural mesothelioma (MPM) is a promising therapeutic strategy. We here investigated the effect of the novel and highly selective Phosphoinositide 3-kinase delta (PI3K-δ) inhibitor roginolisib (IOA-244) on MPM cells and on the immune cells in MPM microenvironment.

To this aim, we analyzed the expression of PI3K-δ by immunohistochemistry in specimens from primary MPM, cell viability and death in three different MPM cell lines treated with roginolisib alone and in combination with ipatasertib (AKT inhibitor) and sapanisertib (mTOR inhibitor). In a co-culture model of patient-derived MPM cells, autologous peripheral blood mononuclear cells and fibroblasts, the tumor cell viability and changes in immune cell composition were investigated after treatment of roginolisib with nivolumab and cisplatin. PI3K-δ was detected in 66/89 (74%) MPM tumors and was associated with reduced overall survival (12 vs. 25 months, P=0.0452). Roginolisib induced apoptosis in MPM cells and enhanced the anti-tumor efficacy of AKT and mTOR kinase inhibitors by suppressing PI3K-δ/AKT/mTOR and ERK1/2 signaling. Furthermore, the combination of roginolisib with chemotherapy and immunotherapy re-balanced the immune cell composition, increasing effector T-cells and reducing immune suppressive cells. Overall, roginolisib induces apoptosis in MPM cells and increases the antitumor immune cell effector function when combined with nivolumab and cisplatin.

These results provide first insights on the potential of roginolisib as a therapeutic agent in patients with MPM and its potential in combination with established immunotherapy regimen.

Abbreviations: ICI, immune checkpoint inhibitor; Treg, T-regulatory; MDSC, myeloid derived suppressor cells; FFPE, formalin-fixed paraffin-embedded; WHO, World Health Organization; TMA, tissue microarrays; IHC, immunohistochemistry; RNA-Seq, RNA sequencing; TCGA, The Cancer Genome Atlas; TPM, transcripts per millions; PBS, phosphate buffered saline; RT, room temperature; BAP, BRCA1-associated protein; FBS, Fetal Bovine Serum; ATCC, American Type Culture Collection; PBMC, peripheral blood mononuclear cells; NK, Natural Killer; iNOS, inducible nitric oxide synthase; Arg, Arginase; CI, combination index; NSCLC, non-small-cell lung cancer; CAFs, cancer associated fibroblasts.

* Corresponding author: Prof Chiara Riganti; Department of Oncology, University of Torino, via Nizza 44, 10126 Torino, Italy; phone:+390116705857
E-mail address: chiara.riganti@unito.it (C. Riganti).

https://doi.org/10.1016/j.tranon.2023.101857
Received 11 June 2023; Received in revised form 12 November 2023; Accepted 3 December 2023
Available online 27 February 2024

Introduction

Malignant pleural mesothelioma (MPM) is a rare and aggressive cancer with limited therapeutic options [1]. A substantial improvement in MPM therapy would require the identification of druggable molecular targets and to overcome resistance mechanisms, including a highly immune-suppressive microenvironment [2,3]. Clinical trials with immune checkpoint inhibitors (ICI), such as nivolumab in combination with ipilimumab, have shown superior overall survival compared to standard of care chemotherapy [4,5]. While ICI have not resulted in significant benefit in MPM, regimen containing ICI may provide a backbone for the development of innovative therapeutic strategies. A promising strategy may consist in combining ICI with molecular targeted therapies, especially when they impair tumor cell intrinsic, tumorigenic signaling pathways [6]. For example, targeting the Phosphoinositide 3-kinase (PI3K) signaling may provide such a novel therapeutic avenue. PI3K belongs to a class of lipid kinase enzymes, some of which were first identified in the late 1980s [7]. Selective inhibitors against the subunit PI3K-δ have emerged as efficient therapeutics against B-cell malignancies [8]. One potent PI3K-δ inhibitor, idelalisib, was approved for the treatment of relapsed B-cell neoplasms, including chronic lymphocytic leukemia, follicular lymphoma, and small lymphocytic leukemia [9]. In addition to their role in hematological malignancies, inhibitors targeting the subunit PI3K-δ have an antitumor effect in solid tumors [10]. The exact mechanisms by which PI3K-δ promotes tumor growth and metastasis are still elusive. One mechanism is thought to rely on the preferential expression of PI3K-δ in T-regulatory (Treg) cells, an immune-suppressive cell population often present in the tumor microenvironment [11]. PI3K-δ inactivation in Treg cells and immune suppressive myeloid derived suppressor cells (MDSC) increases the effector T-cell activity, which in turn induces tumor regression [11,12]. Moreover, up-regulated PI3K-δ expression in tumor cells appears to increase PI3K/AKT signaling in tumor cells, thus directly promoting tumor cell survival and proliferation. Specific PI3K-δ inhibition reversed aberrant PI3K/AKT activation and exhibited antitumor effects in breast cancer [11,12] and Merkel cell carcinoma cells [13,14].

Among the different PI3K-δ inhibitors, roginolisib (IOA-244) is a novel, orally bioavailable small molecule inhibitor that has previously been studied in animal models of autoimmunity and cancer [15,16]. We here investigated for the first time the antitumor activity of roginolisib in MPM models, including its direct activity against tumor cells (i.e., tumor-cell intrinsic activity) and its effect on the tumor microenvironment (i.e., immunomodulatory or extrinsic activity). We found that high dose roginolisib had antitumor effects on MPM cells by suppressing PI3K/AKT signaling activity and inducing apoptosis. Furthermore, roginolisib re-balanced immune cell composition in favor of effector T-cells in a co-culture model mimicking the pleural microenvironment. When roginolisib was combined with specific inhibitors of AKT or mTOR or with cisplatin/nivolumab, we observed an enhanced cytotoxic antitumor effect. Together, these findings provide first evidence for roginolisib as promising therapeutic agent against MPM, especially in combination with established ICI-containing regimen.

Material and methods

Tumor specimens for immunohistochemistry

Formalin-fixed paraffin-embedded (FFPE) resection specimens from 89 patients diagnosed with MPM were analyzed within the frame of this study, including 8 sarcomatoid MPM, 65 epithelioid MPM, and 16 biphasic MPM (Supplemental Table 1). Histological diagnoses were made according to the 2015 World Health Organization (WHO) Classification. The tumor specimens had been extracted from the patients prior chemotherapy and were collected retrospectively. Clinical data of 54 patients could be retrieved from institutional medical records (for 35 patients respective data were not available because they underwent therapy in other institutions). Triplicate 0.6 mm tumor cores were inserted into tissue microarrays (TMA) used for immunohistochemistry (IHC) analysis. Investigations were approved by the Ethics Committee of the University Hospital, Tübingen, Germany (344/2012BO2).

Immunohistochemistry (IHC)

IHC was performed on 3-μM TMA sections and on sections of FFPE-embedded cell lines using conventional 3,3'-diaminobenzidine (DAB) staining on a semi-automated autostainer (LabVision 720, Thermo Fisher Scientific) [17]. After heat-induced epitope retrieval at pH=9, anti-PI3K-δ (D1Q7R, #34050; Cell Signaling, Danvers, MA, USA) (1:1000) was incubated for 30 minutes. PI3K-δ expression was assessed by evaluating the intensity of cytoplasmic staining: 0/no staining; 1+/faint; 2+/moderate; 3+/strong staining in at least 10% tumor cells. Rabbit monoclonal antibody to detect anti-PI3K-δ (D1Q7R) was obtained from Cell Signaling.

Computational analysis of RNA sequencing data from the cancer genome atlas

RNA sequencing (RNA-seq) data (rnaseqv2, level 3) from The Cancer Genome Atlas (TCGA) was downloaded from Firebrowse (http://gdac.broadinstitute.org/) [18]. Transcripts per millions (TPM) were obtained multiplying by 1e6 the normalized expression data ("scaled_estimate"). We considered only data from primary solid tumors. Immune cell fractions were computed from TPM data using the deconvolution method quanTIseq [19] with the following parameter settings: –pipelinestart=decon –tumor=TRUE. Total $CD4^+$ T cells were estimated by summing up conventional ("T.cells.CD4") and regulatory $CD4^+$ T cells ("Tregs"). All analyses and plots were performed in R.

Therapeutic agents

Roginolisib (MW: 584.6 g/mol) was dissolved in dimethyl sulfoxide (DMSO) or in sterile phosphate buffered saline (PBS) at 10 mM. Once resuspended, the solution can be stored at room temperature (RT) in DMSO or at +4C° in PBS for up to 7 days. The suspension was kept in the dark (wrapped in aluminum foil), although the compound itself is not light sensitive. Longer-term storage is possible for 3 months at -20C°. Idelalisib, ipatasertib, sapanisertib (INK128) and paclitaxel were purchased from Selleckchem (Houston, TX, USA). All compounds were diluted in DMSO at 10 mM and then diluted in culture medium at 0.01-10 μM final concentrations. Nivolumab was obtained from SelleckChem and Cisplatin from Sigma-Merck (Milano, Italy).

Cell lines

MPM patient-derived xenograft (PDX) cell lines PXF698 and PXF1118 (both from epithelioid tumors) and PXF1752 (from sarcomatoid MPM) were from Charles River Germany GmbH (Freiburg, Germany) and cultured in RPMI medium supplemented with 10% Fetal Bovine Serum (FBS) (Biochrom AG, Berlin, Germany). Proprietary patient-derived mesothelioma cell lines 420 and 353 were obtained from the Biological Bank of Mesothelioma, Azienda Ospedaliera Nazionale Ss. Antonio e Biagio, Alessandria, Italy (Supplemental Table 2). 420 is a BRCA1-associated protein (BAP)-positive (epithelioid type) primary cell line, and 353 is a BAP-negative (sarcomatoid type) primary cell line. Both cell lines derived from chemonaïve patients. The immunohistochemical characterization had been performed at the Azienda Ospedaliera Universitaria San Luigi Gonzaga, Orbassano, Torino. The mesothelial origin of cells was confirmed by immunostaining of cells fixed in 4% formalin with the following antibodies: calretinin (1:100, rabbit polyclonal #RB-9002-R7, Thermo Fisher Scientific), Wilms tumor-1 antigen (WT1, 1:10, mouse clone 6FH2, Thermo Fisher Scientific), cytokeratin 5 (1:100, mouse clone D5, ImPath, Menarini

Diagnostics), podoplanin (1:150, mouse clone D2-40, Dako), pan-cytokeratin (1:500, mouse clone AE1/AE3, Dako), epithelial membrane antigen (EMA,1:6000, mouse clone E29, Dako), carcinoembryonic antigen (CEA, 1:15000, rabbit polyclonal #IR52661-2, Dako). Cells were cultured in Ham's F12 medium, supplemented with 10% FBS and 1% v/v penicillin-streptomycin. MRC-5 lung fibroblast cell line was purchased from American Type Culture Collection (ATCC) (#CCL-171) and cultured in OptiMEM (Gibco), containing 10% FBS and 1% penicillin-streptomycin. The Ethical Committee of the Biological Bank of Mesothelioma, Ss. Antonio e Biagio Hospital, Alessandria, Italy, and San Luigi Gonzaga Hospital, Orbassano, Italy, approved the study (#126/2016).

Western blotting

Snap-frozen cells were homogenized in lysis buffer (50 mM TRIS-HCl pH 7.6, 250 mM NaCl, 5 mM EDTA, 0.1% Triton X-100) containing complete protease inhibitor cocktail and PhosSTOP phosphatase inhibitor (Roche, Mannheim, Germany) by sonication. Immunoblotting was performed as previously described [20]. Antibodies were used at 1:1.000 dilution, except antibodies against p-AKT and p-RPS6 (1:2.000); β-Actin (1:10.000). Luminescent signals were detected with the digital gel documentation system Stella3200 (Raytest, Straubenhardt, Germany) and quantified using ImageJ 152-win-java8 software (National Institutes of Health, USA). Antibodies to detect PARP1 (46D11, #9532), MCL-1 (D35A5, #5453), BIM (#2819), AKT (C67E7, #4691), p-AKT (S473, D9E, #4060), ERK1/2 (137F5, #4695), p-ERK1/2 (T202/204, #4370), PRAS40 (D23C7, #2691), p-PRAS40 (T246, #2997), RPS6 (5G10, #2217), p-RPS6 (S235/236, #4858) were from Cell Signaling (Danvers, MA, USA). Anti-β-Actin (AC-15) was from Sigma-Aldrich (München, Germany).

Cell viability assay

Cytotoxicity in cell lines was assessed using a 3-(4,5-dimethylthiazol-2-yl)-2,5-diphenyl tetrazolium bromide (MTT)-based assay. Cells were seeded into 96-well plates (4×10^3 cells/100 μl) and incubated with DMSO, roginolisib or idelalisib alone (0.1-100 μM) or in combination with ipatasertib or sapanisertib for 72 h. After addition of 5 mg/ml MTT to each well, the cells were further incubated for 2 h. The produced formazan blue was dissolved in 15% SDS in dimethylformamide-water (1:1), and the absorbance was measured at 550 nm using an EnSpire Multimode Plate Reader 2300 (PerkinElmer). Percent viability was calculated by normalizing absorbance values to those from cells grown in media without drug after background subtraction.

Cell death

For real-time investigation of apoptosis and necrosis, cells were seeded at densities of 1×10^4 cells in 50 μl media into white 96-well plates and incubated for 24 hours at 37°C. Roginolisib (100 μM), paclitaxel (400 nM) or DMSO (0.1%) were added followed by immediate addition of Real Time-Glo Annexin V Apoptosis and Necrosis reagent (part# JA1011, Promega, Madison, WI, USA). Luminescence and fluorescence signals were monitored overtime up to 40 h using the EnSpire Multimode Plate Reader 2300 (PerkinElmer). For end-point investigation of apoptosis and necrosis, cells were seeded at densities of 1×10^5 cells in 1 ml media into 24-well plates and incubated for 24 hours at 37°C. Then, cells were treated with roginolisib (100 μM) or DMSO (0.1%) and incubated for a further 31 hours. After harvesting using accutase, cells were stained using Annexin V-APC (Immunotools, Friesoythe, Germany) and 25 μg/ml PI (propidium iodide) for 10 min. Cells were analysed by a BD FACSLyric Flow Cytometry System (BD, Heidelberg, Germany). Phase-contrast microscopy was used to investigate morphological changes. Cells (1×10^5 cells/2ml) were seeded into 6-well plates and incubated with roginolisib (100 μM) or DMSO for 24 h. Cells were imaged using a CKX41 inverted microscope and Olympus CellF (Olympus Life Science, Tokyo, Japan).

Caspase 3/7 activity assay

Caspase activity was detected using a Caspase-Glo 3/7 assay kit (Promega) according to the manufacturer's protocol. Cells (1×10^4 cells/50μl) were seeded into 96-well plates and incubated for 24 hours at 37°C. Cells were treated with roginolisib or DMSO (0.1%) and assayed after 24 hours. Briefly, plates and caspase 3/7 reagent were allowed to equilibrate at room temperature, reagent was then added to wells at a 1:1 ratio and incubated for 30 min at room temperature. Luminescence was measured using the VICTOR Nivo microplate reader (Perkin Elmer). Caspase activity was calculated by normalizing luminescence values to those from cells grown in media without drug after background subtraction.

Viability in MPM-fibroblast co-cultures

5×10^5 patient derived MPM cells and 1×10^5 MRC-5 cells were seeded in 24 μl MaxGel ECM (Sigma-Merck) and maintained for 48 hours in complete Ham's F12 medium. Peripheral blood mononuclear cells (PBMCs) obtained from the peripheral blood of the corresponding MPM patient by centrifugation on Ficoll-Hypaque density gradient were added at a 1:10 ratio with target (i.e., MPM) cells and kept in culture for further 5 days. After this incubation time, cells were immunophenotyped (Supplemental Figure 1). Roginolisib (0.025 μM, corresponding to the IC50 of MPM 420 and 353, co-cultured with MRC-5 cells) was added either alone or in combination with cisplatin (5 μM) and/or nivolumab (1 μg/ml). Each concentration corresponds to the IC_{50} of MPM 420 and 353. Two different treatment schedules were used: (a) combined/concomitant administration of roginolisib with cisplatin+nivolumab for 72 h; (b) sequential treatment of initial cisplatin+nivolumab for 48 h, followed by roginolisib for 24 h. In both schedules the drugs were added in the last 72 hours to MPM-MRC5 cells co-cultured with PBMC. Cell viability was measured by WST-1 reagent (Sigma-Merck), as per manufacturer's instructions.

Apoptosis assay (propidium iodide/annexin-V-assay) in MPM-fibroblast co-cultures

An Annexin V-FITC Kit (Milteny Biotec) was used to measure the induction of apoptosis in MPM-fibroblast co-cultures. Cells were prepared as previously described [21] and Annexin V staining was accomplished according to the manufacturer's instructions. After staining, the cells were analyzed using a CytoFlex (Beckman Coulter, Brea, CA, USA). Data were analyzed with the Kaluza® Flow Analysis Software (Beckman Coulter, Brea, CA, USA). Apoptotic cell status according to treatment schedule (concomitant and subsequent) were performed using the nonparametric Kruskal–Wallis test followed by Dunn's multiple comparison test. The P values <0.05 were considered statistically significant. Each data point represents the mean value of percentage of positive cells obtained in 4 independent experiments for each cell line. Statistical analyses were carried out by GraphPad Prism 8 (GraphPad Software Inc., San Diego, CA).

Immunophenotyping

PBMC were collected from the supernatant, washed and re-suspended in PBS containing 5% v/v FBS. A three- and four-color flow cytometry was performed on 1×10^6 cells, by combining the following antibodies (all diluted 1:10, Miltenyi Biotec., if not indicated otherwise) for: CD3 (REA613), CD4 (mouse clone M-T466), CD8 (mouse clone BW135/80) for T-lymphocytes; CD4 (mouse clone M-T466), FoxP3 (REA1253) for Treg cells; CD56 (mouse clone AF127H3), CD335/NKp46 (mouse clone 9E2) for Natural Killer (NK) cells; CD19 (REA675) for B-lymphocytes; CD68 (mouse clone Y1/82A), CD86 (REA268) and

inducible nitric oxide synthase (iNOS, mouse clone 51CB52, BioLegend) for M1-polarized macrophages, CD68 (mouse clone Y1/82A), CD206 (mouse clone DCN228) and Arginase (Arg; mouse clone 14D2C43, BioLegend) for M2-polarized macrophages; CD11b (rat clone M1/70.15.11.5), CD15 (mouse clone VIMC6), CD14 (mouse clone TUK4) for Granulocytic (Gr) and Monocytic (Mo) MSDC. The amount of activated $CD8^+$T-cells was measured by staining $CD8^+$T-cells with anti-Ki67 (REA183) as index of proliferation and with anti-IFN-γ (REA600) as index of antitumor activation. For the detection of immune checkpoint markers on $CD4^+/CD8^+$T-lymphocytes and/or immune checkpoint ligands on MPM cells, cells were washed twice with ice-cold PBS, detached with Cell Dissociation solution (Sigma-Merck) and re-suspended in PBS containing 5% FBS. Marker proteins were detected using antibodies for CD279/PD-1 (mouse clone PD1.3.1.3), CD223/LAG-3 (mouse clone REA351), CD366/TIM-3 (mouse clone F38-2E2), CD152/CTLA-4 (mouse clone BNI3; all diluted 1:10, Miltenyi Biotec.), CD274/PD-L1 (1:1,000, mouse clone 29E.2A3, BioLegend). 1×10^5 cells were analyzed using a Guava EasyCyte flow cytometer (Millipore), equipped with the InCyte software.

Statistical analysis

The statistical tests were done using GraphPad Prism 8.0 (GraphPad Software Inc., San Diego, CA). The test used, number of samples and significance are indicated in the respective figure legends. P-values of < 0.05 were considered statistically significant. The CompuSyn software was used for generating a combination index (CI) of drug combinations [22,23].

Patients consent

Written informed consent was obtained from the patient for publication of this study and accompanying images. A copy of the written consent is available for review by the Editor-in-Chief of this journal on request.

Results

PI3K-δ protein expression is associated with reduced overall survival of MPM patients

Protein expression of PI3K-δ in primary MPM specimens was assessed in a cohort of 89 patients. Immunostaining revealed up-regulated expression of PI3K-δ protein (moderate or strong immunostaining) in 74% (66/89) of samples (Fig. 1A and Supplemental Table 1). PI3K-δ expression was independent of the type of MPM, the age and gender of the patients and did not correlate with TNM stages (Table 1). Patients with moderate/strong PI3K-δ expression, however, had shorter overall survival compared to patients with negative/weak expression (12 months vs. 25 months, respectively; P = 0.0452) (Table 1, Fig. 1B). The high prevalence of PI3K-δ expression in primary MPM prompted us to investigate the therapeutic efficacy and the mechanism of action of

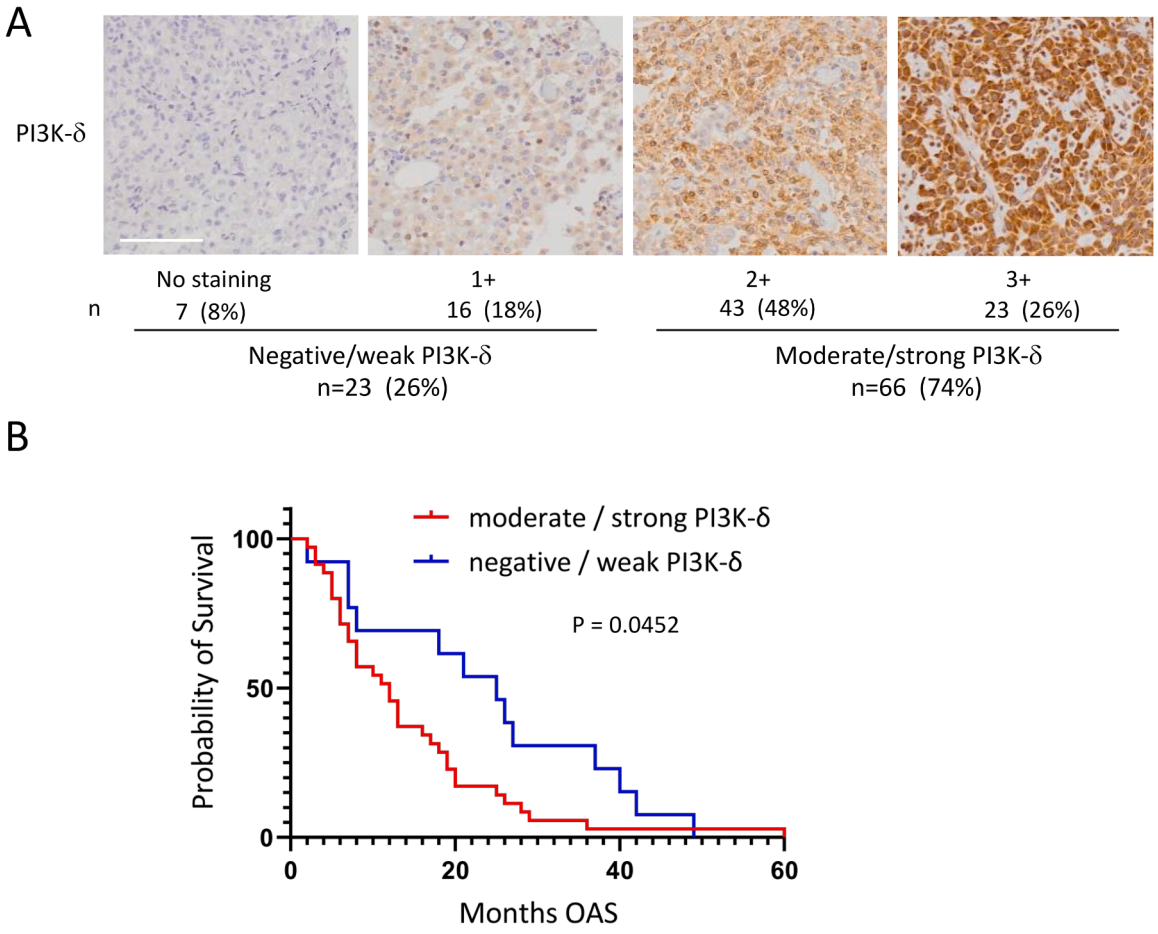

Fig. 1. PI3K-δ protein expression: characteristics and clinical impact on the survival of MPM patients. (A) PI3K-δ protein expression in 89 primary MPM specimens was assessed by evaluating the intensity of cytoplasmic immunostaining: 0/no staining; 1+/faint; 2+/moderate; 3+/strong staining in at least 10% tumor cells. Scale, 100 μm. (B) Patients with moderate/strong PI3K-δ expression had a shorter overall survival (OAS) compared to those with negative/weak expression (12 vs. 25 months, respectively; Log-rank (Mantel-Cox) test, P=0.0452). Survival data were available for 51 patients (n=14 no/low, n=37 moderate/high PI3K-δ). Survival was calculated from time of diagnosis.

Table 1
Association between PI3K-δ expression and clinicopathological characteristics in 89 MPM patients.

	Variable	Total (n=89)	PI3K-δ expression No/Low (n=21)	Moderate/ High (n=68)	P value
Age (year)					0.417
	Median	72	72	71	
	Range	51-90	62-83	51-90	
Gender					0.468
	Male	80	18 (85.7%)	62 (91.2%)	
	Female	9	3 (14.3%)	6 (8.8%)	
Histological type					0.292
	Epithelioid	66	17 (81.0%)	49 (72.1%)	
	Sarcomatoid	8	2 (9.5%)	6 (8.8%)	
	Biphasic	15	2 (9.5%)	13 (19.1%)	
T stage*					0.201
	T1 + T2	23	8 (57.1%)	15 (37.5%)	
	T3 + T4	31	6 (42.9%)	25 (62.5%)	
M stage*					0.751
	M0	49	13 (92.9%)	36 (90.0%)	
	≥ M1	5	1 (7.1%)	4 (10.0%)	
N stage*					0.347
	N0	37	11 (78.6%)	26 (65.0%)	
	≥ N1	17	3 (21.4%)	14 (35.0%)	
Overall survival (months)**					0.045
	Median	13	25	12	
	Range	2-145	2-145	2-111	

* TNM stages were available for 54 patients (n=14 no/low, n=40 moderate/high PI3K-δ)
** Survival was calculated from time of diagnosis. Data were available for 51 patients (n=14 no/low, n=37 moderate/high PI3K-δ).

the specific PI3K-δ inhibitor roginolisib in MPM cell lines as well as in primary MPM cells in a co-culture model.

The PI3K-δ inhibitor roginolisib induces apoptotic cell death in MPM cells

To assess the direct effect on tumor cells, we investigated whether treatment of three MPM cell lines (PXF698, PXF1118, PXF1752) with roginolisib would affect the survival, proliferation, cell death and intracellular PI3K/AKT/mTOR signaling of MPM cells. All three cell lines expressed PI3K-δ, albeit at a lower level than primary MPM tumors (Fig. 2A). First, the cytotoxic efficacy of roginolisib was analyzed by exposing MPM cells to increasing concentrations (0.1-100 μM) of the drug for 72 hours, after which cell viability was assessed by an MTT assay. Roginolisib impaired cell viability and proliferation in all three cell lines independent of the histological subtype, leading to a reduction of cell viability by 34-60% (Fig. 2A).

The mechanism of cell death induced by roginolisib in MPM cells was investigated in PXF1752 and PXF698 cells. We measured the exposure of phosphatidylserine at the outer leaflet of the plasma membrane by annexin V binding as well as the loss of membrane integrity by cellular uptake of a fluorescent membrane-impermeable DNA stain in real-time over 40 hours (PXF698) and by using a flow-cytometry based end-point assay (both cell lines). Apoptotic cell death is characterized by a delay between phosphatidylserine translocation and the loss of membrane integrity, whereas necrotic cell death is defined by concomitant annexin V binding and loss of membrane integrity. Roginolisib induced an apoptotic signature in PXF698 cells with a clear temporal lag between phosphatidylserine exposure and loss of membrane integrity of 14 hours while DMSO did not induce cell death within 40 hours (Fig. 2B). As a control, we used paclitaxel to induce canonical apoptotic cell death. Consistently, end-point investigation revealed an accumulation of PXF698 and PXF1752 cells in early apoptosis (annexin-V positive - PI negative cells), while an increase in necrotic cells (annexin-V positive - PI positive cells) was not detectable at the same time-points (Supplemental Fig. 2A and 3A). Of note, reduced roginolisib concentrations resulted in delayed induction of apoptosis: when 100 μM roginolisib were applied to PXF698 and PXF1752 cells, apoptotic cells were observed after 16-24 hours and 31 hours, respectively, while 10 μM roginolisib induced apoptosis detectable in both cell lines at 48 hours (Fig. 2B, Supplemental Fig. 2A and 3A). Induction of apoptosis was confirmed by apoptotic membrane blebbing (Fig. 2D, Supplemental Fig. 2B), enhanced caspase-3/7 activity (Fig. 2C, Supplemental Fig. 2C and 3B), and cleavage of the caspase substrate PARP1 (Fig. 2E). In both cell lines, the amount of pro-apoptotic BIM and MCL-1 remained unaffected during 24-hour roginolisib exposure, indicating BIM-independent apoptosis (Fig. 2E).

On the molecular level, PI3K/AKT/mTOR signaling was inhibited in a dose- and time-dependent manner (Fig. 2F, Supplemental Fig. 2D): decreased AKT (Ser473) and S6RP (S235/236) phosphorylation was observed upon 4 hour-exposure in PXF1752 and PXF1118 cells. Furthermore, roginolisib treatment inhibited phosphorylation of ERK1/2 (T202/204), a key-regulator of cell survival and proliferation interconnected with the PI3K/AKT signaling pathway (Fig. 2G), in PXF1118 cells (Fig. 2F).

Roginolisib enhances the antitumor efficacy of AKT and mTOR inhibitors

Simultaneous inhibition of PI3K-δ and AKT or PI3K-δ and mTOR by treatment with roginolisib or, for the purpose of comparison, with the well-characterized PI3K-δ inhibitor idelalisib in combination with ipatasertib (pan-AKT inhibitor) or sapanisertib (mTORC1/mTORC2 inhibitor) resulted in an enhanced inhibition of cell viability in MPM cells compared to each drug individually (Fig. 3A, Supplemental Fig. 4), because of the crosstalk between these pathways (Fig. 3B). Analysis using the CompuSyn CI algorithm showed that the decline in cell viability was strongly synergistic at a wide range of concentrations in PXF698, PXF1118 and PXF1752 cells (all co-expressing PI3K-δ, AKT and mTOR), with the only exception of combined idelalisib/ipatasertib therapy of PXF1752 cells (Supplemental Fig. 4 A-D).

Protein levels of phosphorylated AKT (S473), PRAS40 (T246), RPS6 (S235/236) and ERK1/2 (T202/204) were quantified in PXF1118 and PXF1752 cells by immunoblotting to determine AKT, mTOR and ERK activity upon combination therapy (Fig. 3C, Supplemental Fig. 5). Ipatasertib alone induced AKT phosphorylation in a similar manner as other ATP-competitive AKT inhibitors that protect Ser473 from phosphatases, leading to increased p-AKT [24]. Despite this increase in p-AKT, downstream AKT signaling activity was inhibited, indicated by decreased p-PRAS and p-S6RP levels after 4 hours of treatment. Inhibition of mTORC1/mTORC2 by sapanisertib resulted in a decrease of p-AKT, p-PRAS40 and p-S6RP. Roginolisib and idelalisib both enhanced the inhibitory effect of ipatasertib and sapanisertib on AKT, which resulted in robust dephosphorylation of PRAS40 and S6RP. Furthermore, ERK1/2 phosphorylation was substantially decreased upon PI3K-δ/AKT and PI3K-δ/mTOR inhibition. Notably, the effect of idelalisib on AKT and ERK signaling was even stronger than that observed for roginolisib corresponding to the greater impact of idelalisib (as single agent and in combination) on the viability of MPM cells (Fig. 3A). Regarding the potential clinical impact of PI3K-δ/AKT and PI3K-δ/mTOR targeted therapy, we observed simultaneously up-regulated expression of PI3K-δ and at least one AKT isoform in 75% (61/81) patient tumors and of PI3K-δ and mTOR in 20% (17/84) MPM (Supplemental Table 1).

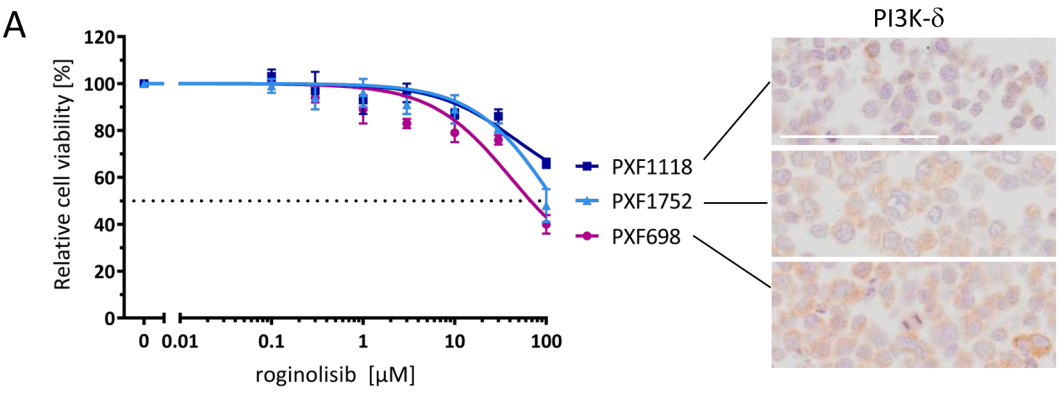

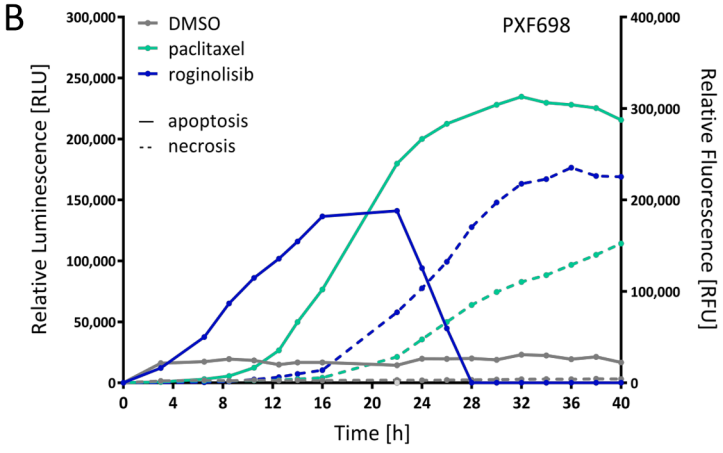

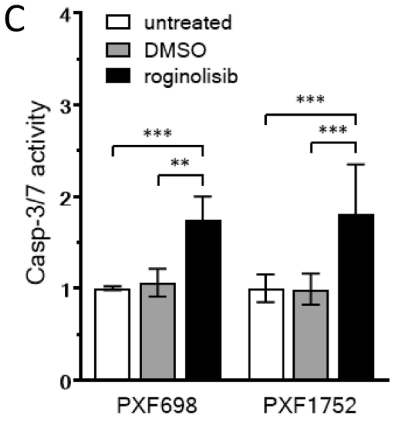

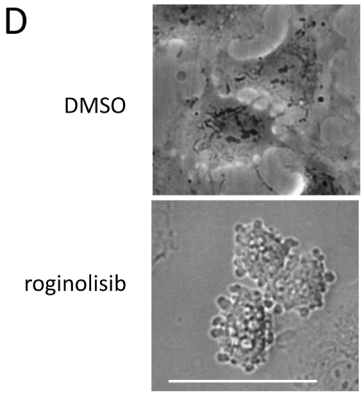

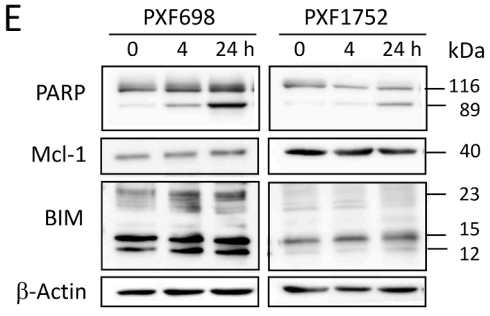

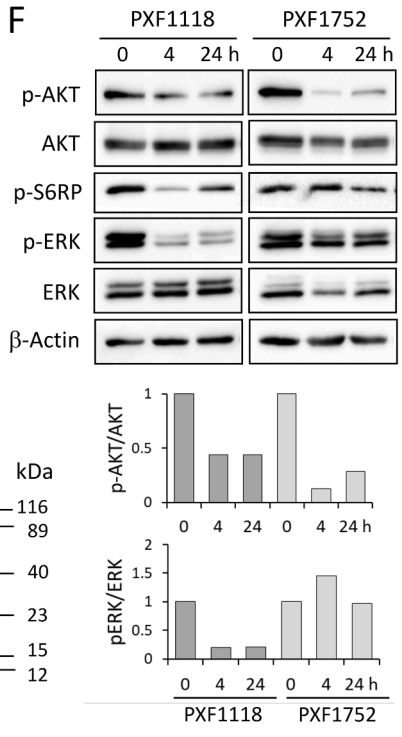

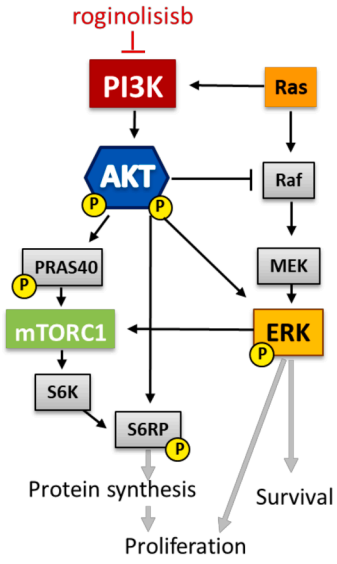

(caption on next page)

Fig. 2. Roginolisib impairs mesothelioma cell viability and induces apoptotic cell death. (A) MPM cell lines PXF698, PXF1118 and PXF1752 were exposed to the indicated concentrations of roginolisib. The viability of the cells was measured after 72 h of treatment by a MTT cytotoxicity assay. Data points, mean ± SD of independent triplicate experiments. Immunohistochemistry analysis of PI3K-δ protein expression in PXF698, PXF1118 and PXF1752 cells. Scale, 50 μm. (B) PXF698 cells were exposed to roginolisib (100 μM), paclitaxel (400 nM) or DMSO in the presence of the RealTime-Glo Annexin V Apoptosis and Necrosis Assay. Luminescence (phosphatidylsprrerine:annexin V binding – apoptosis; solid line) and fluorescence (loss of membrane integrity – necrosis; dashed line) were recorded for 40 h at the indicated time points. A clear temporal lag between phosphatidylserine exposure and lack of membrane integrity is indicative of apoptotic cell death leading to secondary necrosis. Data points, mean of duplicate samples, representative of independent duplicate experiments. (C) Caspase-3/7 activity after treatment of cells with 100 μM roginolisib or 0.1% DMSO for 24 h. Data points, mean ± SD of independent triplicate experiments. 2way ANOVA test (Dunnett's multiple comparison); ****, p<0.0001; ***, p=0.0002. (D) Apoptotic membrane blebbing after treatment of PXF698 cells with 100 μM roginolisib for 24 h, detected by phase-contrast microscopy. (E) PARP cleavage and levels of Mcl-1 and BIM in PXF698 and PXF1752 cells after 100 μM roginolisib treatment at 0, 4, 24 h. (F) Immunoblotting shows the levels of p-AKT (S473) and p-ERK1/2 (T202/204) in PXF1118 and PXF1752 cells after 100 μM roginolisib treatment at 0, 4, 24 h. Bar graphs represent semi-quantitative analysis of phospho-protein expression relative to total protein, normalized to protein levels at 0 h. (G) Schematic illustration of PI3K/AKT/mTOR and ERK signaling.

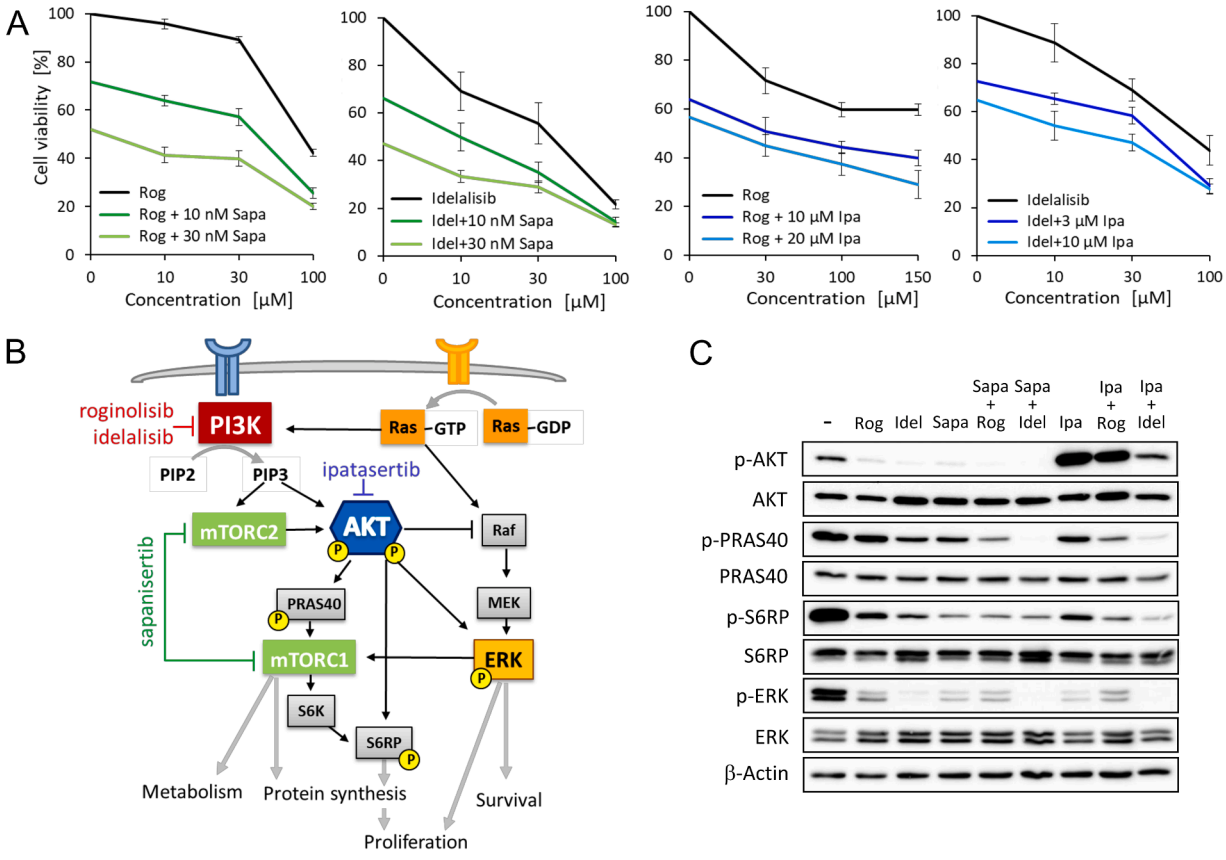

Fig. 3. Synergistic cytotoxicity of PI3K-δ inhibitors and sapanisertib (mTORC1/2 inhibitor) or ipatasertib (AKT inhibitor). (A) MPM cells were treated with PI3K-δ inhibitors roginolisib (Rog) or idelalisib (Idel) as single agents and in combination with sapanisertib (Sapa) (PXF698) or ipatasertib (Ipa) (PXF1118) for 72 h, after which cell viability was assessed using an MTT cytotoxicity assay. Data points, mean of quintuplets of two independent experiments. (B) Schematic illustration of PI3K/AKT/mTOR and ERK signaling. Growth factors and hormones activate PI3 kinase catalyzing the production of PIP3, which in turn coordinates cell proliferation, metabolism and survival via activating AKT and mTOR signaling pathways. mTOR kinase serves as core component of two distinct protein complexes, mTORC1 and mTORC2. Activated Ras triggers both PI3K/AKT and ERK signaling, regulating cell proliferation and survival. (C) Molecular effects of simultaneous PI3K-δ/mTOR and PI3K-δ/AKT inhibition. Immunoblotting shows the levels of p-AKT (S473), p-PRAS40 p-PRAS40 (T246), p-RPS6 (S235/236) and p-ERK1/2 (T202/204) in PXF1118 cells treated with 100 μM roginolisib (Rog), 100 μM idelalisib (Idel), 30 nM sapanisertib (Sapa), 10 μM ipatasertib (Ipa), or their combinations as indicated for 4 h.

PIK3CD gene expression correlates with an abundance of T-regulatory cells and M2 macrophages

In order to assess the correlation between PIK3CD gene expression and the presence of different immune cell subpopulations in MPM tumors, we used RNA sequencing (RNA-seq) data from 87 primary MPM samples from TCGA [18] and analyzed them with the quanTIseq deconvolution tool [19]. We found that PIK3CD gene expression was not correlated with Treg cell abundance (Fig 4). Instead, there was a weak, but significant, positive correlation of PIK3CD with $CD8^+$T-cells and M2 macrophages (Fig 4). For comparison, we used similar data for non-small-cell lung cancer (NSCLC), where the correlation between PIK3CD and Treg cells, M1 and M2 macrophages was strong and significant in both adenocarcinoma and squamous cell carcinoma (Supplemental Fig 6 and 7).

Roginolisib exerts immunomodulatory activity

For further studies on immunomodulatory activity we focused on roginolisib alone because idelalisib, although being more effective against tumor cells, causes severe adverse effects while roginolisib is well tolerated in patients. We further investigated the role of roginolisib

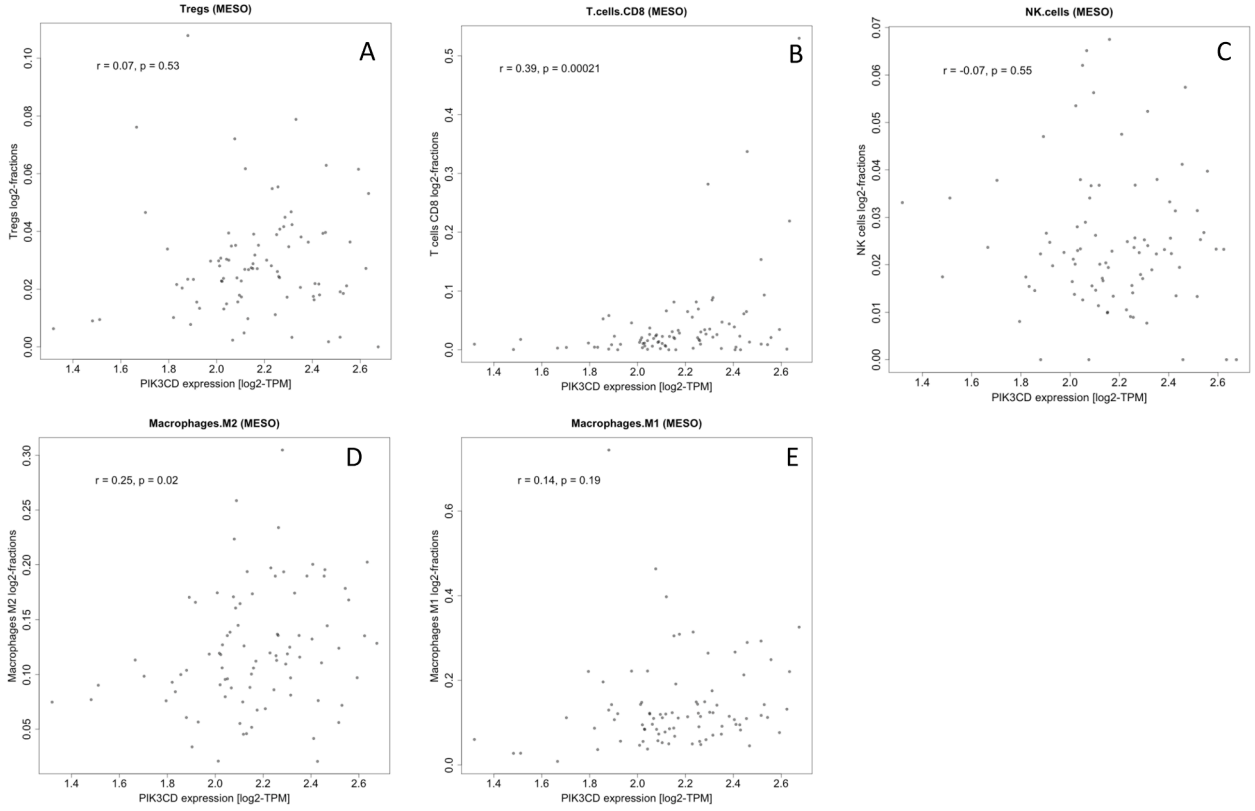

Fig. 4. PIK3CD gene expression correlates with the abundance of CD8$^+$ T cells and M2 macrophages in MPM tumors. PIK3CD gene expression data from TCGA data sets (n=87 MPM samples) were plotted against an immune profile for Tregs (A), CD8$^+$ T-cells (B), NK cells (C), M2 macrophages (D) and M1 macrophages (E). r, correlation coefficient; p, p-value.

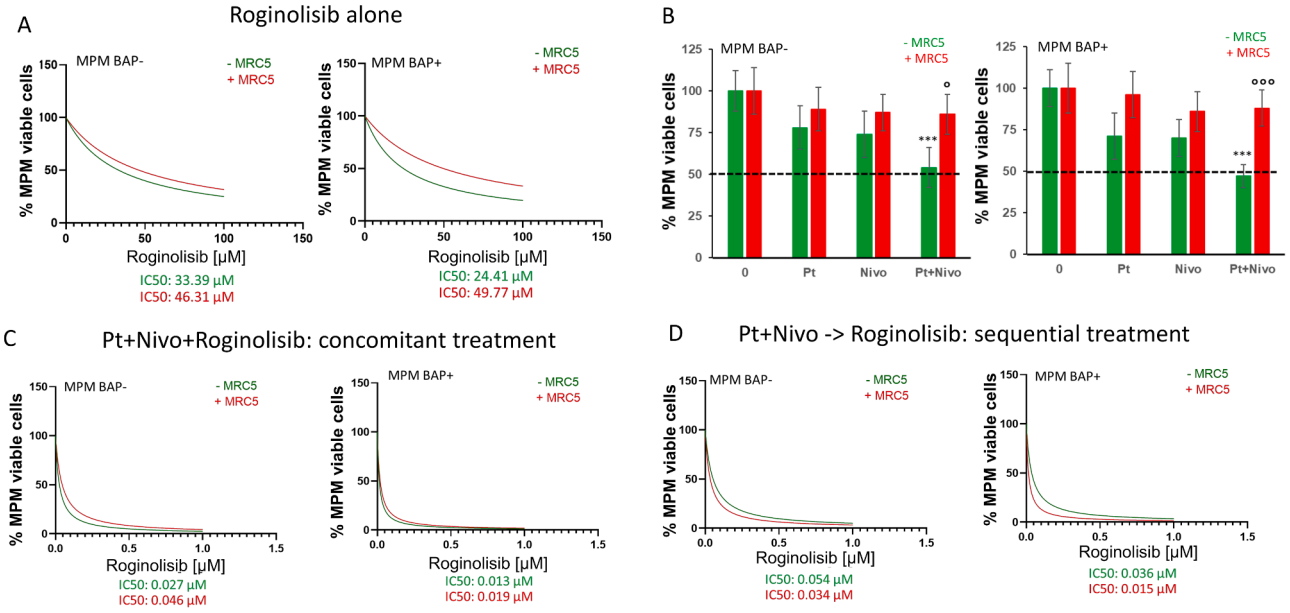

Figure 5. Roginolisib enhances the cytotoxicity of cisplatin and nivolumab in patient-derived tumor cells in the presence of stromal cells. (A) BAP1-wild-type epithelioid (BAP$^+$ epi) and BAP1-null sarcomatoid (BAP$^-$ sar) MPM cells were co-cultured with peripheral mononuclear cells (PBMCs) and exposed to the indicated concentrations of roginolisib in the absence (-MRC5) or presence of fibroblasts (+MRC5). The viability of the cells was measured after 72 hours by WST-1 staining. Data points, mean of independent quadruplicate experiments. (B) MPM cells were treated with 5 µM cisplatin (Pt) and 1 µg/ml nivolumab (Nivo) for 72 h in the absence and presence of MRC5 cells. (C, D) The combination of roginolisib with 5 µM cisplatin plus 1 µg/ml nivolumab, either as combined/concomitant treatment (C) or in sequential treatment (D), was investigated in the absence (-MRC5) and presence of fibroblasts (+MRC5). 0: untreated cells. Nonparametric Kruskal–Wallis test followed by Dunn's multiple comparison test; ***p<0.001: vs. untreated cells; °p<0.05, °°°p<0.001: MRC5+ vs MRC5-.

by creating a co-culture MPM model consisting of patient tumor cells, MRC-5 lung fibroblasts and patient-matched PBMCs (Supplemental Fig. 1). Roginolisib treatment for 72 hours impaired the viability of patient-derived tumor cells, achieving a reduction of cell viability of 75-80% (Fig. 5A). Interestingly, addition of MRC-5 cells increased the viability of MPM cells when treated with roginolisib alone (Fig. 5A). This stromal protection was even more pronounced when a combination of cisplatin and PD1 monoclonal antibody nivolumab was applied: co-culture with MRC-5 cells reduced the effect of cisplatin/nivolumab to 15% compared to 50% efficacy in the absence of fibroblasts (Fig. 5B). This protective effect was impaired when cisplatin, nivolumab and roginolisib were applied together, either concomitantly or sequentially (Fig. 5D). We also noticed that increasing concentrations of roginolisib improved cytotoxicity of cisplatin/nivolumab (Fig. 5B-D).

Of note, immune cells derived from patient matched PBMCs and used in the co-culture showed distinct changes within their subsets.

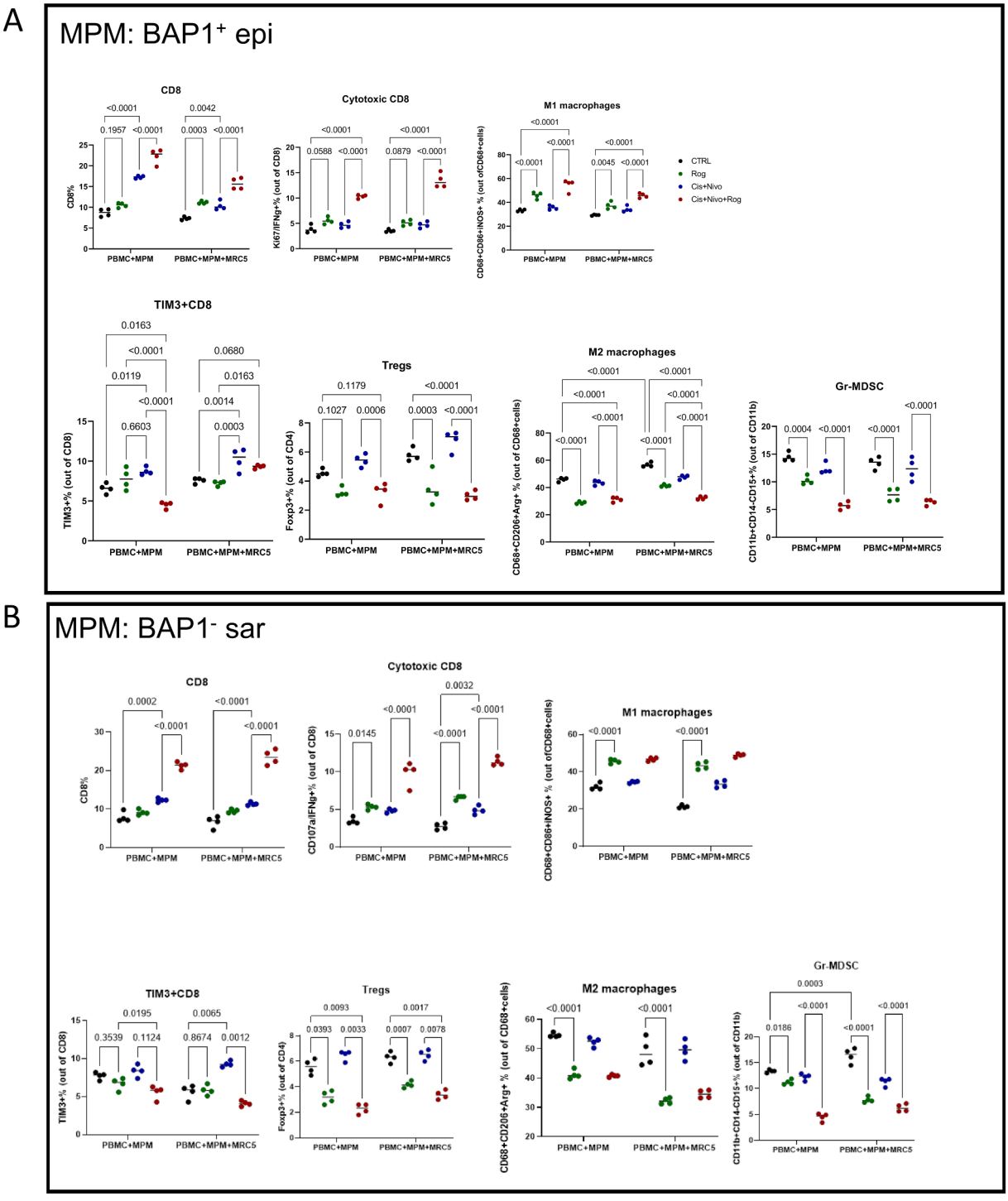

Figure 6. Roginolisib exerts immunomodulatory activity. BAP1-wild-type epithelioid (A) and BAP1-null sarcomatoid (B) MPM cells were co-cultured with peripheral mononuclear cells (PBMCs) in the absence or presence of MRC5 fibroblasts and treated with roginolisib alone, co-incubated with cisplatin/nivolumab or in sequential treatment (cisplatin/nivolumab followed by roginolisib). The immunophenotype of immune cells was analyzed by flow cytometry (n = 2, two independent experiments). *p<0.05, **p<0.01, ***p<0.001.

Treatment with roginolisib alone and roginolisib in combination with cisplatin/nivolumab resulted in the up-regulation of cytotoxic $CD8^+$T-lymphocytes and M1 macrophages, and in the reduction of Tregs, M2 macrophages and Gr-MDSCs (Fig. 6A and 6B). Moreover, sequential treatment with roginolisib after cisplatin/nivolumab induced an accumulation of proliferating (i.e., $Ki67^+$) and activated (i.e., IFN-γ^+) $CD8^+$T-cells which also expressed lower PD-1 and TIM3 on their cell surface (Fig. 6A and 6B). The therapeutic and immunomodulatory effects of roginolisib as single agent were similar in BAP1-wild-type and BAP1-null MPM and independent of the histological MPM subtype. However, in combination with cisplatin/nivolumab roginolisib was more efficient in BAP1-wild-type than in BAP1-null models (sequential treatment, IC50 0.015 μM vs. 0.034 μM).

Discussion

The PI3K/AKT/mTOR signaling network is involved in cell proliferation, survival, metabolism, motility and immunity [25]. Aberrant activation of this pathway is observed in several types of cancer, including MPM [26,27]. Until recently, the PI3K/AKT/mTOR pathway was targeted with isoform unselective agents resulting in unsatisfactory benefit/risk profiles, especially in MPM, where single-digit overall response rates were accompanied by considerable toxicities [28–31]. Therefore, recent drug development has focused on PI3K isoform-specific inhibitors, such as roginolisib (IOA-244). Roginolisib is a novel, oral and highly selective inhibitor of the PI3K-δ subunit. Contrasting with prior PI3K-δ inhibitors, roginolisib is a non-ATP competitive allosteric modulator that achieves a confirmational change of the inactive PI3K-δ subunit [15,16]. Our present work shows that roginolisib exerts antitumor activity in mesothelioma experimental models by targeting both cancer cells and immune cells in the microenvironment.

This study, to our knowledge, is the first report demonstrating constitutive activation of PI3K-δ in MPM. Aberrant PI3K-δ protein expression was observed in 74% archival MPM tumors and shown to be associated with shorter survival of the patients. When added to MPM tumor cells expressing PI3K-δ, roginolisib blocked PI3K/AKT/mTOR signaling, which resulted in the inhibition of proliferation and survival, and the induction of apoptosis. This effect was similar to the one previously reported for PI3K-δ inhibitors IC87114 and idelalisib in breast cancer [11,12] and Merkel cell carcinoma [13,14], respectively. Consistent with other PI3K inhibitors, the cell killing efficacy of roginolisib was modest as a single agent [11–13]. Once roginolisib was simultaneously administered with mTOR or AKT inhibitors, MPM cell survival was reduced: roginolisib and idelalisib were significantly more cytotoxic when combined either with the AKT inhibitor ipatasertib or the mTOR inhibitor sapanisertib, suggesting a cooperative effect to inactivate PI3K/AKT/mTOR signalling. Since co-activation of the respective target molecules is frequent in MPM tumors – 75% MPM cases showed up-regulated expression of PI3K-δ/AKT, and 20% MPM expressed PI3K-δ/mTOR – combined roginolisib/ipatasertib and roginolisib/sapanisertib therapies are promising therapy options potentially suitable for large numbers of MPM patients, and thus should be further evaluated *in vivo* and in clinical studies.

While roginolisib is highly selective at concentrations below 100 μM [16], the effects *in vitro* were most significant at doses of 100 μM. Hence, we cannot exclude that a certain inhibition of PI3Kβ may have contributed to the antitumor effect. Furthermore, those high roginolisib concentrations would be beyond clinical relevance. It is, however, conceivable that roginolisib will be effective in MPM patients at lower concentrations, i.e. below 10 μM: i) The majority of patient tumors express the target molecule PI3K-δ at significantly higher levels than the cell lines used in this study. For a lot of drugs, sensitivity correlates with the expression level of the targets these drugs are directed against [32]. ii) *In vitro* administration of roginolisib was limited to 72 hours while in patients the drug is being given over a period of several weeks. The concept of a longer administration of the drug at lower concentrations is supported by our observation that treatment with reduced roginolisib concentrations of 10 μM still resulted in significant, albeit delayed, induction of apoptosis. iii) In patients with advanced melanoma, roginolisib achieved partial response and stable disease at C_{max} concentration levels between 5 and 10 μM (NCT04328844). iv) In addition to inducing tumor cell apoptosis, roginolisib increases the antitumor immune cell effector function. Hence, roginolisib was active at lower concentrations in our co-culture models, in particular when applied together with cisplatin/nivolumab (IC50 <0.1 μM).

Deletion of the tumor suppressor NF2 gene is a key genomic alteration implicated in the pathogenesis of MPM [26]. NF2 inactivation leads to aberrant activation of mTOR, which in turn activates oncogenic protein, lipid and nucleotide synthesis, cell proliferation and survival [26,33]. Inhibition of mTOR by rapamycin and its derivatives suppressed MPM cell growth in pre-clinical models [33–35], but was not effective in clinical trials (NCT01024946) [36]. The poor response to rapamycin derivatives is, at least in part, caused by an adverse AKT activation triggered by release of the negative feedback from mTOR to PI3K [37]. Here, we observed that both roginolisib and idelalisib acted synergistically with the dual mTORC1/mTORC2 inhibitor sapanisertib, almost completely inhibiting AKT and the downstream AKT signaling (PRAS40, S6RP). Further, simultaneous PI3K-δ/mTOR inhibition blocked the interconnected ERK1/2 signaling, which together resulted in profound suppression of MPM cell survival.

Idelalisib impaired MPM tumor cell growth more profoundly than roginolisib. For further studies on the immunomodulatory activity, we focused on roginolisib because idelalisib is known to generate unspecific metabolites *in vivo* [38] resulting in severe adverse effects, such as diarrhea and serious infections [39]. In contrast, roginolisib was well tolerated with an acceptable side-effect profile in a clinical phase 1 study (NCT04328844) achieving partial response (n=2/18) and stable disease in advanced uveal and cutaneous melanoma patients [40,41]. Hence, roginolisib appears to have a greater translational potential than idelalisib or other prior PI3K inhibitors.

Cisplatin/pemetrexed and immune checkpoint inhibitors have only modestly extended survival in MPM due to multiple mechanisms of resistance. Key contributors to resistance are Tregs and macrophages. For example, high infiltration of immune-suppressive Tregs and macrophages in solid tumors are associated with hyperprogression and resistance to current therapy, including immune checkpoint inhibitors [3,42-44]. To investigate the impact of roginolisib on immune cells, we used a co-culture model that has a unique advantage over standard in vivo animal experiments, because it relies on autologous human immune cells, mimicking the interface between MPM and immune-environment better than syngeneic mice, whose immune cells have different functional pathways, or humanized mice that are heterologous models. Our data show that PI3K-δ inhibition by roginolisib decreased the number of Tregs and M2 macrophages in the co-culture MPM model and enhanced the cytotoxicity of cisplatin/nivolumab. Moreover, sequential treatment with roginolisib after cisplatin/nivolumab induced an accumulation of cytotoxic T-cells. Our data suggest that roginolisib, by disrupting the function of immunosuppressing cells (Tregs, macrophages) and activating cytotoxic T cells, has the potential to induce effective antitumour immunity and thus to sensitize MPM to cisplatin and immune checkpoint inhibitors.

Our data are consistent with prior observations showing that PI3K-δ inactivation has exerted antitumor activity in other solid tumors: pharmacological PI3K-δ inhibition in breast cancer xenografts induced depletion of tumor-associated macrophages which reduced tumor growth and metastasis [11,12]; genetic PI3K-δ inactivation decreased Tregs in xenograft models of solid tumors [45]. Although Tregs are dependent on PI3K-δ for proliferation signals [11] we failed to find a correlation between PIK3CD gene expression and the abundance of Treg cells in MPM tumors using RNA-seq data of a small cohort of MPM tumors deposited in the TCGA databank. By contrast, PI3K-δ inhibition with roginolisib significantly decreased the number of Tregs in our

co-culture MPM models indicating that there is a potential connection between PI3K-δ activity and Treg cell abundance.

We observed a correlation of $CD8^+$T-cells with PIK3CD expression in MPM and, more importantly, that PI3K-δ inhibition forced the accumulation of active (i.e., IFN-γ^+) $CD8^+$ T-cells. This was mainly observed in the sequential treatment, i.e., when roginolisib was applied after cisplatin/nivolumab. Thus, combining ICIs with blockade of PIK3-δ might sensitize tumors to immunotherapy, by addressing T-cell mediated antitumor immunity at multiple points: (1) increase in active $CD8^+$ T-cells, (2) reduction of Tregs and (3) reactivation of T-cell function by blocking PD-1. Roginolisib enhanced the antitumor effect of cisplatin/nivolumab therapy in our MPM models. Similar to our observations, combined therapy of the PI3K inhibitor parsaclisib and pembrolizumab led to increased T cell activity and IFN-γ signaling [46].

Another mechanism of resistance is mediated by cancer associated fibroblasts (CAFs), which protect tumor cells through cell-to-cell contacts, secretion of stromal factors, and metabolic interactions [47]. We observed a reduction in the efficacy of nivolumab/cisplatin when primary MPM cells were cultured in the presence of fibroblasts. This protective effect disappeared when roginolisib was added in combination or two days after nivolumab/cisplatin therapy (i.e., as part of the sequential treatment). It is conceivable that roginolisib suppressed pro-survival PI3K/AKT signaling mediated by stromal CAFs, thus sensitizing MPM cells to cisplatin/nivolumab therapy. Sarcomatoid histology and loss of tumor suppressor BAP1 are associated with poor response to chemotherapy in MPM patients [48,49]. The effects of PI3K-δ inhibition on tumor cell survival and immune cell abundance that we show here were irrespective of histology and BAP1 status. Moreover, cisplatin/nivolumab therapy was improved by roginolisib in both MPM models, without and with BAP1 loss, albeit in the latter at higher drug concentrations. Together, our data suggest that roginolisib therapy might also be suitable for critical MPM subgroups, i.e. sarcomatoid MPM and BAP1-loss MPM.

Conclusions

PI3K-δ is widely expressed in MPM, and pharmacological inactivation of PI3K-δ in experimental MPM models has antitumor activity by targeting both cancer cells and immune cells in the tumor microenvironment (Supplemental Fig. 8). This study provides for the first time evidence to support the use of the specific PI3K-δ inhibitor roginolisib in combination therapies for MPM and other malignancies.

Declaration of competing interest

The authors declare the following financial interests/personal relationships which may be considered as potential competing interests:

Claudia Kalla, German Ott and Roger Falkenstern-Ge received Roginolisib from iOnctura SA and grants from iOnctura SA, Charles River Germany GmbH and Robert Bosch Stiftung (grant project 704 to CK, GO and RG-G); Francesca Finotello received grants from iOnctura SA; Karolina Niewola-Staszkowska, Giusy di Conza, Michael Lahn and Lars van der Veen are employees of iOnctura SA; Michael Lahn and Lars van der Veen are the stock owner of Roginolisib; Julia Schueler received funding from Charles River Germany GmbH; Joanna Kopecka received funding from Fondazione Cassa di Rispoarmio di Torino (grant 2021); Chiara Riganti received Roginolisib from iOnctura SA and grants from from iOnctura SA, and Italian Association for Cancer Research (IG 21480).

Funding

This work was supported by the Robert Bosch Stiftung, Stuttgart, Germany (Project 704), Fondazione Cassa di Risparmio di Torino (ID2020.1648); Italian Association for Cancer Research (IG21408). The funding bodies had no role in the collection, analysis, interpretation of the data, manuscript writing and decision to submit the manuscript for publication.

Acknowledgments

We thank Katja Bräutigam, IKP Stuttgart, for expert technical assistance.

Supplementary materials

Supplementary material associated with this article can be found, in the online version, at doi:10.1016/j.tranon.2023.101857.

References

[1] M. Cinausero, K. Rihawi, F. Sperandi, B. Melotti, A. Ardizzoni, Chemotherapy treatment in malignant pleural mesothelioma: a difficult history, J. Thorac Dis. 10 (Suppl 2) (2018) S304–S310.
[2] R. Bueno, E.W. Stawiski, L.D. Goldstein, S. Durinck, A. De Rienzo, Z. Modrusan, F. Gnad, T.T. Nguyen, B.S. Jaiswal, L.R. Chirieac, D. Sciaranghella, N. Dao, C. E. Gustafson, K.J. Munir, J.A. Hackney, A. Chaudhuri, R. Gupta, J. Guillory, K. Toy, C. Ha, Y.J. Chen, J. Stinson, S. Chaudhuri, N. Zhang, T.D. Wu, D.J. Sugarbaker, F. J. de Sauvage, W.G. Richards, S. Seshagiri, Comprehensive genomic analysis of malignant pleural mesothelioma identifies recurrent mutations, gene fusions and splicing alterations, Nat. Genet 48 (4) (2016) 407–416.
[3] J. Minnema-Luiting, H. Vroman, J. Aerts, R. Cornelissen, Heterogeneity in Immune Cell Content in Malignant Pleural Mesothelioma, Int. J. Mol. Sci. 19 (4) (2018).
[4] P. Baas, A. Scherpereel, A.K. Nowak, N. Fujimoto, S. Peters, A.S. Tsao, A. S. Mansfield, S. Popat, T. Jahan, S. Antonia, Y. Oulkhouir, Y. Bautista, R. Cornelissen, L. Greillier, F. Grossi, D. Kowalski, J. Rodriguez-Cid, P. Aanur, A. Oukessou, C. Baudelet, G. Zalcman, First-line nivolumab plus ipilimumab in unresectable malignant pleural mesothelioma (CheckMate 743): a multicentre, randomised, open-label phase 3 trial, Lancet 397 (10272) (2021) 375–386.
[5] S. Peters, A. Scherpereel, R. Cornelissen, Y. Oulkhouir, L. Greillier, M.A. Kaplan, T. Talbot, I. Monnet, S. Hiret, P. Baas, A.K. Nowak, N. Fujimoto, A.S. Tsao, A. S. Mansfield, S. Popat, X. Zhang, N. Hu, D. Balli, T. Spires, G. Zalcman, First-line nivolumab plus ipilimumab versus chemotherapy in patients with unresectable malignant pleural mesothelioma: 3-year outcomes from CheckMate 743, Ann. Oncol. 33 (5) (2022) 488–499.
[6] P. Gotwals, S. Cameron, D. Cipolletta, V. Cremasco, A. Crystal, B. Hewes, B. Mueller, S. Quaratino, C. Sabatos-Peyton, L. Petruzzelli, J.A. Engelman, G. Dranoff, Prospects for combining targeted and conventional cancer therapy with immunotherapy, Nat. Rev. Cancer 17 (5) (2017) 286–301.
[7] S.A. Courtneidge, A. Heber, An 81 kd protein complexed with middle T antigen and pp60c-src: a possible phosphatidylinositol kinase, Cell 50 (7) (1987) 1031–1037.
[8] N. Tzenaki, E.A. Papakonstanti, p110delta PI3 kinase pathway: emerging roles in cancer, Front Oncol. 3 (2013) 40.
[9] B.W. Miller, D. Przepiorka, R.A. de Claro, K. Lee, L. Nie, N. Simpson, R. Gudi, H. Saber, S. Shord, J. Bullock, D. Marathe, N. Mehrotra, L.S. Hsieh, D. Ghosh, J. Brown, R.C. Kane, R. Justice, E. Kaminskas, A.T. Farrell, R. Pazdur, FDA approval: idelalisib monotherapy for the treatment of patients with follicular lymphoma and small lymphocytic lymphoma, Clin. Cancer Res. 21 (7) (2015) 1525–1529.
[10] F. Janku, T.A. Yap, F. Meric-Bernstam, Targeting the PI3K pathway in cancer: are we making headway? Nat. Rev. Clin. Oncol. 15 (5) (2018) 273–291.
[11] S. Ahmad, R. Abu-Eid, R. Shrimali, M. Webb, V. Verma, A. Doroodchi, Z. Berrong, R. Samara, P.C. Rodriguez, M. Mkrtichyan, S.N. Khleif, Differential PI3Kdelta Signaling in CD4(+) T-cell Subsets Enables Selective Targeting of T Regulatory Cells to Enhance Cancer Immunotherapy, Cancer Res. 77 (8) (2017) 1892–1904.
[12] E. Goulielmaki, M. Bermudez-Brito, M. Andreou, N. Tzenaki, M. Tzardi, E. de Bree, E. Tsentelierou, A. Makrigiannakis, E.A. Papakonstanti, Pharmacological inactivation of the PI3K p110delta prevents breast tumour progression by targeting cancer cells and macrophages, Cell Death Dis. 9 (6) (2018) 678.
[13] B. Fang, A. Kannan, S. Zhao, Q.H. Nguyen, S. Ejadi, M. Yamamoto, J. Camilo Barreto, H. Zhao, L. Gao, Inhibition of PI3K by copanlisib exerts potent antitumor effects on Merkel cell carcinoma cell lines and mouse xenografts, Sci. Rep. 10 (1) (2020) 8867.
[14] M.B. Shiver, F. Mahmoud, L. Gao, Response to Idelalisib in a Patient with Stage IV Merkel-Cell Carcinoma, N. Engl. J. Med. 373 (16) (2015) 1580–1582.
[15] P. Haselmayer, M. Camps, M. Muzerelle, S. El Bawab, C. Waltzinger, L. Bruns, N. Abla, M.A. Polokoff, C. Jond-Necand, M. Gaudet, A. Benoit, D. Bertschy Meier, C. Martin, D. Gretener, M.S. Lombardi, R. Grenningloh, C. Ladel, J.S. Petersen, P. Gaillard, H. Ji, Characterization of Novel PI3Kdelta Inhibitors as Potential Therapeutics for SLE and Lupus Nephritis in Pre-Clinical Studies, Front Immunol 5 (2014) 233.
[16] Z. Johnson, C. Tarantelli, E. Civanelli, L. Cascione, F. Spriano, A. Fraser, P. Shah, T. Nomanbhoy, S. Napoli, A. Rinaldi, K. Niewola-Staszkowska, M. Lahn, D. Perrin, M. Wenes, D. Migliorini, F. Bertoni, L. van der Veen, G. Di Conza, IOA-244 is a non-ATP-competitive, highly selective, tolerable phosphoinositide 3-kinase delta inhibitor that targets solid tumors and breaks immune tolerance, Cancer Research Communications (2023).

[17] K. Gruber, M. Kohlhaufl, G. Friedel, G. Ott, C. Kalla, A novel, highly sensitive ALK antibody 1A4 facilitates effective screening for ALK rearrangements in lung adenocarcinomas by standard immunohistochemistry, J. Thorac. Oncol. 10 (4) (2015) 713–716.
[18] N. Cancer Genome Atlas Research, J.N. Weinstein, E.A. Collisson, G.B. Mills, K. R. Shaw, B.A. Ozenberger, K. Ellrott, I. Shmulevich, C. Sander, J.M. Stuart, The Cancer Genome Atlas Pan-Cancer analysis project, Nat. Genet. 45 (10) (2013) 1113–1120.
[19] F. Finotello, C. Mayer, C. Plattner, G. Laschober, D. Rieder, H. Hackl, A. Krogsdam, Z. Loncova, W. Posch, D. Wilflingseder, S. Sopper, M. Ijsselsteijn, T.P. Brouwer, D. Johnson, Y. Xu, Y. Wang, M.E. Sanders, M.V. Estrada, P. Ericsson-Gonzalez, P. Charoentong, J. Balko, N. de Miranda, Z. Trajanoski, Molecular and pharmacological modulators of the tumor immune contexture revealed by deconvolution of RNA-seq data, Genome Med. 11 (1) (2019) 34.
[20] D. Monch, S. Bode-Erdmann, J. Kalla, J. Strater, C. Schwanen, R. Falkenstern-Ge, S. Klumpp, G. Friedel, G. Ott, C. Kalla, A subgroup of pleural mesothelioma expresses ALK protein and may be targetable by combined rapamycin and crizotinib therapy, Oncotarget 9 (29) (2018) 20781–20794.
[21] I. Vermes, C. Haanen, H. Steffens-Nakken, C. Reutelingsperger, A novel assay for apoptosis. Flow cytometric detection of phosphatidylserine expression on early apoptotic cells using fluorescein labelled Annexin V, J. Immunol Methods 184 (1) (1995) 39–51.
[22] N. Zhang, J.N. Fu, T.C. Chou, Synergistic combination of microtubule targeting anticancer fludelone with cytoprotective panaxytriol derived from panax ginseng against MX-1 cells in vitro: experimental design and data analysis using the combination index method, Am. J. Cancer Res. 6 (1) (2016) 97–104.
[23] T.C. Chou, Theoretical basis, experimental design, and computerized simulation of synergism and antagonism in drug combination studies, Pharmacol Rev. 58 (3) (2006) 621–681.
[24] Y.C. Lin, H.C. Kuo, J.S. Wang, W.W. Lin, Regulation of inflammatory response by 3-methyladenine involves the coordinative actions on Akt and glycogen synthase kinase 3beta rather than autophagy, J. Immunol. 189 (8) (2012) 4154–4164.
[25] L. Yu, J. Wei, P. Liu, Attacking the PI3K/Akt/mTOR signaling pathway for targeted therapeutic treatment in human cancer, Semin Cancer Biol. 85 (2022) 69–94.
[26] T. Sato, Y. Sekido, NF2/Merlin Inactivation and Potential Therapeutic Targets in Mesothelioma, Int. J. Mol. Sci. 19 (4) (2018).
[27] Y. Suzuki, H. Murakami, K. Kawaguchi, T. Tanigushi, M. Fujii, K. Shinjo, Y. Kondo, H. Osada, K. Shimokata, Y. Horio, Y. Hasegawa, T. Hida, Y. Sekido, Activation of the PI3K-AKT pathway in human malignant mesothelioma cells, Mol. Med. Rep. 2 (2) (2009) 181–188.
[28] J.C. Bendell, A.M. Varghese, D.M. Hyman, T.M. Bauer, S. Pant, S. Callies, J. Lin, R. Martinez, E. Wickremsinhe, A. Fink, V. Wacheck, K.N. Moore, A First-in-Human Phase 1 Study of LY3023414, an Oral PI3K/mTOR Dual Inhibitor, in Patients with Advanced Cancer, Clin. Cancer Res. 24 (14) (2018) 3253–3262.
[29] S.O. Dolly, A.J. Wagner, J.C. Bendell, H.L. Kindler, L.M. Krug, T.Y. Seiwert, M. G. Zauderer, M.P. Lolkema, D. Apt, R.F. Yeh, J.O. Fredrickson, J.M. Spoerke, H. Koeppen, J.A. Ware, J.O. Lauchle, H.A. Burris, J.S. de Bono, Phase I Study of Apitolisib (GDC-0980), Dual Phosphatidylinositol-3-Kinase and Mammalian Target of Rapamycin Kinase Inhibitor, in Patients with Advanced Solid Tumors, Clin. Cancer Res. 22 (12) (2016) 2874–2884.
[30] M.G. Zauderer, E.W. Alley, J. Bendell, E. Capelletto, T.M. Bauer, S. Callies, A. M. Szpurka, S. Kang, M.D. Willard, V. Wacheck, A.M. Varghese, Phase 1 cohort expansion study of LY3023414, a dual PI3K/mTOR inhibitor, in patients with advanced mesothelioma, Invest New Drugs 39 (4) (2021) 1081–1088.
[31] B. Chmielowski, R.J. Sullivan, M. Postow, A. Patnaik, G. Shapiro, E. Cohen, M. Gutierrez, C. Steuer, A. Ribas, L. Lee, B. O'Connell, J. Kutok, J. Roberts, S. Mahabhashyam, M.-L. Fjallskog, J.D. Wolchok, D. Hong, The first clinical/translational data from the expansion cohorts of a Ph1/1b Study of IPI-549, a tumor macrophage-reprogramming small molecule, in: in combination with nivolumab in advanced solid tumors. Poster 716, Annual Meeting Society for Immunotherapy of Cancer, Journal for ImmunoTherapy of Cancer, Washington DC, 2018.
[32] R. Roy, L.N. Winteringham, T. Lassmann, A.R.R. Forrest, Expression Levels of Therapeutic Targets as Indicators of Sensitivity to Targeted Therapeutics, Mol. Cancer Ther. 18 (12) (2019) 2480–2489.
[33] M.A. Lopez-Lago, T. Okada, M.M. Murillo, N. Socci, F.G. Giancotti, Loss of the tumor suppressor gene NF2, encoding merlin, constitutively activates integrin-dependent mTORC1 signaling, Mol. Cell Biol. 29 (15) (2009) 4235–4249.
[34] M.L. Hartman, J.M. Esposito, B.Y. Yeap, D.J. Sugarbaker, Combined treatment with cisplatin and sirolimus to enhance cell death in human mesothelioma, J. Thorac. Cardiovasc Surg. 139 (5) (2010) 1233–1240.
[35] M.A. Hoda, A. Mohamed, B. Ghanim, M. Filipits, B. Hegedus, M. Tamura, J. Berta, B. Kubista, B. Dome, M. Grusch, U. Setinek, M. Micksche, W. Klepetko, W. Berger, Temsirolimus inhibits malignant pleural mesothelioma growth in vitro and in vivo: synergism with chemotherapy, J Thorac. Oncol. 6 (5) (2011) 852–863.
[36] S.H. Ou, J. Moon, L.L. Garland, P.C. Mack, J.R. Testa, A.S. Tsao, A.J. Wozniak, D. R. Gandara, SWOG S0722: phase II study of mTOR inhibitor everolimus (RAD001) in advanced malignant pleural mesothelioma (MPM), J. Thorac. Oncol 10 (2) (2015) 387–391.
[37] X. Wan, B. Harkavy, N. Shen, P. Grohar, L.J. Helman, Rapamycin induces feedback activation of Akt signaling through an IGF-1R-dependent mechanism, Oncogene 26 (13) (2007) 1932–1940.
[38] C.M. Chen, W.B. Wu, J.F. Chen, Y. Chen, Characterization of the in vitro metabolites of idelalisib in liver microsomes and interspecies comparison, J. Pharm Biomed. Anal 162 (2019) 249–256.
[39] I. Hus, B. Pula, T. Robak, PI3K inhibitors for the treatment of chronic lymphocytic leukemia: current status and future perspectives, Cancers (Basel) 14 (6) (2022).
[40] A.M. Di Giacomo, F. Santangelo, G. Amato, E. Simonetti, J. Graham, M. Lahn, L. van der Veen, Z. Johnson, C. Pickering, M. Durini, Z. Tan, T. Lakshmikanth, P. Brodin, M. Occhipinti, M. Simonelli, C. Carlo-Stella, A. Santoro, P. Spiliopoulou, T.R.J. Evans, M. Maio, First-in-human (FIH) phase I study of the highly selective phosphoinositide 3-kinase inhibitor delta (PI3Kδ) inhibitor IOA-244 in patients with advanced cancer: Safety, activity, pharmacokinetic (PK), and pharmacodynamic (PD) results. Abstract 3107. ASCO Annual Meeting, J. Clin. Oncol. Chicago, ASCO, 2022, p. 2022.
[41] C. Carlostella, M. Lahn, T. Hammett, L. van der Veen, Z. Johnson, C. Pickering, A. Santoro, P1116: safety, pharmacokinetic (pk), pharmacodynamic (pd) and activity of the highly selective phosphoinositide 3-kinase inhibitor delta (pi3kδ) inhibitor ioa-244 in patients with follicular lymphoma (fl), in: E.H. Association (Ed.), HemaSphere, Vienna, Annual Meeting, 2022.
[42] H. Wakiyama, T. Kato, A. Furusawa, R. Okada, F. Inagaki, H. Furumoto, H. Fukushima, S. Okuyama, P.L. Choyke, H. Kobayashi, Treg-dominant tumor microenvironment is responsible for hyperprogressive disease after PD-1 blockade therapy, Cancer Immunol Res. (2022).
[43] D.R. Principe, L. Chiec, N.A. Mohindra, H.G. Munshi, Regulatory T-Cells as an Emerging Barrier to Immune Checkpoint Inhibition in Lung Cancer, Front Oncol 11 (2021) 684098.
[44] B.Z. Qian, J.W. Pollard, Macrophage diversity enhances tumor progression and metastasis, Cell 141 (1) (2010) 39–51.
[45] K. Ali, D.R. Soond, R. Pineiro, T. Hagemann, W. Pearce, E.L. Lim, H. Bouabe, C. L. Scudamore, T. Hancox, H. Maecker, L. Friedman, M. Turner, K. Okkenhaug, B. Vanhaesebroeck, Inactivation of PI(3)K p110delta breaks regulatory T-cell-mediated immune tolerance to cancer, Nature 510 (7505) (2014) 407–411.
[46] J.M. Kirkwood, N. Iannotti, D. Cho, S. O'Day, G. Gibney, F.S. Hodi, P. Munster, P. Hoyle, S. Owens, M. Smith, N. Mettu, Abstract CT176: effect of JAK/STAT or PI3Kδ plus PD-1 inhibition on the tumor microenvironment: biomarker results from a phase Ib study in patients with advanced solid tumors, Cancer Research 78 (13_Supplement) (2018) CT176.
[47] P.E. Saw, J. Chen, E. Song, Targeting CAFs to overcome anticancer therapeutic resistance, Trends Cancer 8 (7) (2022) 527–555.
[48] A.S. Mansfield, J.T. Symanowski, T. Peikert, Systematic review of response rates of sarcomatoid malignant pleural mesotheliomas in clinical trials, Lung Cancer 86 (2) (2014) 133–136.
[49] K. Oehl, B. Vrugt, U. Wagner, M.B. Kirschner, M. Meerang, W. Weder, E. Felley-Bosco, B. Wollscheid, K. Bankov, M.C. Demes, I. Opitz, P.J. Wild, Alterations in BAP1 Are Associated with Cisplatin Resistance through Inhibition of Apoptosis in Malignant Pleural Mesothelioma, Clin. Cancer Res. 27 (8) (2021) 2277–2291.

Supplemental materials

Supplemental Table 1: Protein expression of PI3K-δ, AKT and mTOR in 89 MPM specimens

						Immunohistochemistry data		
MPM specimen	**Histology***	**Gender**	**Age at diagnosis**	**TNM**	**Overall survival****	**Protein expression**§		
					[months]	**PI3K-δ**	**AKT**#	**mTOR**#
MPM11	S	M	75	T3N3M0	3	moderate	moderate	weak
MPM12	S	F	73	not available	not available	moderate	moderate	no
MPM13	S	M	81	T3N0M0	8	moderate	moderate	no
MPM14	S	M	69	T3N2M2	8	strong	moderate	weak
MPM15	S	M	77	not available	not available	moderate	moderate	no
MPM18	S	M	76	not available	not available	no	weak	no
MPM20	E	F	62	T2N0M0	not available	weak	moderate	weak
MPM21	E	M	73	T2N2M0	13	strong	moderate	weak
MPM22	E	M	59	T1N0M0	17	strong	moderate	no
MPM23	E	M	57	T3N0M0	10	strong	moderate	weak
MPM24	E	M	65	T1N0M0	40	weak	moderate	moderate
MPM26	E	M	74	T3N0M0	13	strong	moderate	moderate
MPM27	E	M	71	T3N0M0	19	moderate	moderate	no
MPM28	E	M	70	T2N0M0	26	moderate	moderate	moderate
MPM29	E	M	73	T3N2M0	36	moderate	moderate	moderate
MPM30	E	F	68	T2N0M0	60	moderate	moderate	moderate
MPM32	E	M	72	T3N0M0	49	weak	moderate	moderate
MPM33	E	M	76	T1N0M0	12	moderate	moderate	moderate
MPM34	E	M	51	T3N0M0	20	strong	moderate	moderate
MPM36	E	M	76	T4N2M2	26	weak	moderate	moderate
MPM37	E	M	86	T1N0M0	2	strong	moderate	moderate
MPM40	E	M	62	T3N2M0	11	strong	weak	n.a.

MPM41	E	M	72	T3N0M0	21	no	moderate	weak
MPM43	E	M	86	T3N0M0	3	moderate	moderate	moderate
MPM44	E	M	75	T3N2M0	8	weak	moderate	weak
MPM45	E	M	73	T2N0M0	28	moderate	moderate	weak
MPM46	E	M	64	T2N0M0	25	moderate	moderate	no
MPM47	E	F	83	T3N1M0	6	moderate	moderate	weak
MPM48	E	F	76	T3N0M0	6	moderate	moderate	weak
MPM49	E	M	66	T2N0M0	7	weak	moderate	weak
MPM50	E	M	72	T3N0M0	37	weak	moderate	moderate
MPM51	E	F	77	T3N0M0	not available	moderate	moderate	moderate
MPM53	E	F	65	T3N1M0	2	no	n.a.	n.a.
MPM54	E	F	69	T2N0M0	25	weak	moderate	no
MPM55	E	M	80	T2N0M0	29	strong	moderate	weak
MPM56	B	M	79	T4N0M0	4	moderate	moderate	weak
MPM58	B	M	58	T2N0M0	20	strong	moderate	weak
MPM59	B	M	64	not available	not available	strong	moderate	weak
MPM60	B	M	68	T3N2M0	5	moderate	moderate	weak
MPM62	B	M	63	T4N0M0	19	moderate	moderate	weak
MPM63	B	M	62	T4N2M1	5	moderate	moderate	weak
MPM66	E	M	75	not available	not available	moderate	moderate	weak
MPM67	B	M	70	T2N2M0	not available	strong	moderate	weak
MPM68	E	M	86	not available	not available	moderate	n.a.	no
MPM69	E	M	75	not available	not available	weak	n.a.	weak
MPM71	E	M	75	not available	not available	weak	moderate	moderate
MPM72	E	F	81	not available	not available	moderate	moderate	weak
MPM73	E	M	81	not available	not available	moderate	moderate	weak
MPM74	E	M	59	not available	not available	moderate	moderate	no
MPM75	E	M	80	not available	not available	moderate	moderate	moderate
MPM79	E	M	75	not available	not available	weak	moderate	weak
MPM81	E	M	72	not available	not available	weak	moderate	weak

MPM82	E	M	75	not available	not available	no	moderate	no
MPM85	E	M	81	not available	not available	no	n.a.	no
MPM88	E	M	75	not available	not available	moderate	moderate	moderate
MPM90	E	M	61	T3N0M0	8	strong	moderate	moderate
MPM91	E	M	55	T2N0M0	not available	moderate	moderate	no
MPM93	E	M	76	T2N0M0	18	no	moderate	n.a.
MPM94	B	M	64	T2N2M1	not available	strong	moderate	weak
MPM95	S	M	83	T2N0M0	7	weak	moderate	no
MPM97	E	M	54	T4N3M0	16	strong	moderate	weak
MPM98	E	M	65	T4N0M0	12	moderate	moderate	weak
MPM99	B	M	67	T2N0M0	42	weak	moderate	weak
MPM100	B	M	69	T2N0M0	27	no	moderate	weak
MPM101	E	M	66	not available	not available	moderate	moderate	weak
MPM102	E	M	75	T3N2M0	7	strong	n.a.	n.a.
MPM103	E	M	68	not available	not available	strong	moderate	weak
MPM104	E	M	72	T3N0M0	13	moderate	moderate	weak
MPM105	E	M	58	T4N2M2	6	strong	moderate	weak
MPM106	B	M	65	T1N0M0	18	moderate	moderate	moderate
MPM107	B	M	70	T3N2M0	5	strong	moderate	weak
MPM108	E	M	66	T3N0M0	7	moderate	moderate	weak
MPM109	E	M	66	not available	not available	moderate	moderate	weak
MPM113	B	M	85	not available	not available	moderate	moderate	weak
MPM114	E	M	65	T1N0M0	not available	moderate	moderate	no
MPM115	E	M	71	not available	not available	moderate	moderate	moderate
MPM118	B	M	87	not available	not available	moderate	moderate	weak
MPM121	E	M	55	not available	not available	moderate	moderate	moderate
MPM122	E	M	74	not available	not available	strong	moderate	weak
MPM123	E	M	71	not available	not available	moderate	moderate	weak
MPM124	S	M	74	not available	not available	weak	n.a.	n.a.

MPM126	B	M	76	not available	not available	strong	moderate	weak
MPM127	E	M	69	not available	not available	weak	moderate	weak
MPM128	E	M	77	not available	not available	moderate	moderate	weak
MPM129	E	M	64	not available	not available	strong	moderate	moderate
MPM130	E	M	90	not available	not available	strong	moderate	weak
MPM131	E	M	76	not available	not available	moderate	n.a.	weak
MPM133	E	M	55	not available	not available	moderate	n.a.	moderate
MPM134	B	M	71	not available	not available	moderate	moderate	weak

n.a.; not analyzed

* S, sarcomatoid; E, epithelioid; B, biphasic (epitheloid and sarcomatoid components)

** Survival calculated from time of diagnosis

§ Moderate and strong staining were regarded as up-regulated protein expression.

Data from Kalla et al. (manuscript in preparation)

Supplemental Table 2: Characterization of Primary Mesothelioma Cells 420 and 353 by immunohistochemical analysis (WHO Classification 2015/2021) and clinical information

Expression - Targets		**Cell 420**	**Cell 353**
	Abbreviation	epithelioid type	sarcomatoid type
Calretinin	CALR	+	-
Pan-Cytokeratin	PANCK	+	+
Podoplanin	PODO	-	-
Epithelial Membrane Antigen	EMA	-	-
Carcinoembryonic Antigen	CEA	-	-
Wilms Tumor 1	WT1	+	-
Cytokeratin 5	CK5	+	+
BRCA-associated protein 1	BAP-1	+	-
Clinical information		**Patient 420**	**Patient 353**
Age		79	80
Sex		M	F
Stage		III	III
Surgery		No	No
Neo-adjuvant chemotherapy		No	No
First line adjuvant chemotherapy		carboplatin+pemetrexed	carboplatin+pemetrexed
Second line adjuvant chemotherapy		pemetrexed	none
OS (months)		27	7

OS: overall survival calculated from time of diagnosis

Supplemental Figures

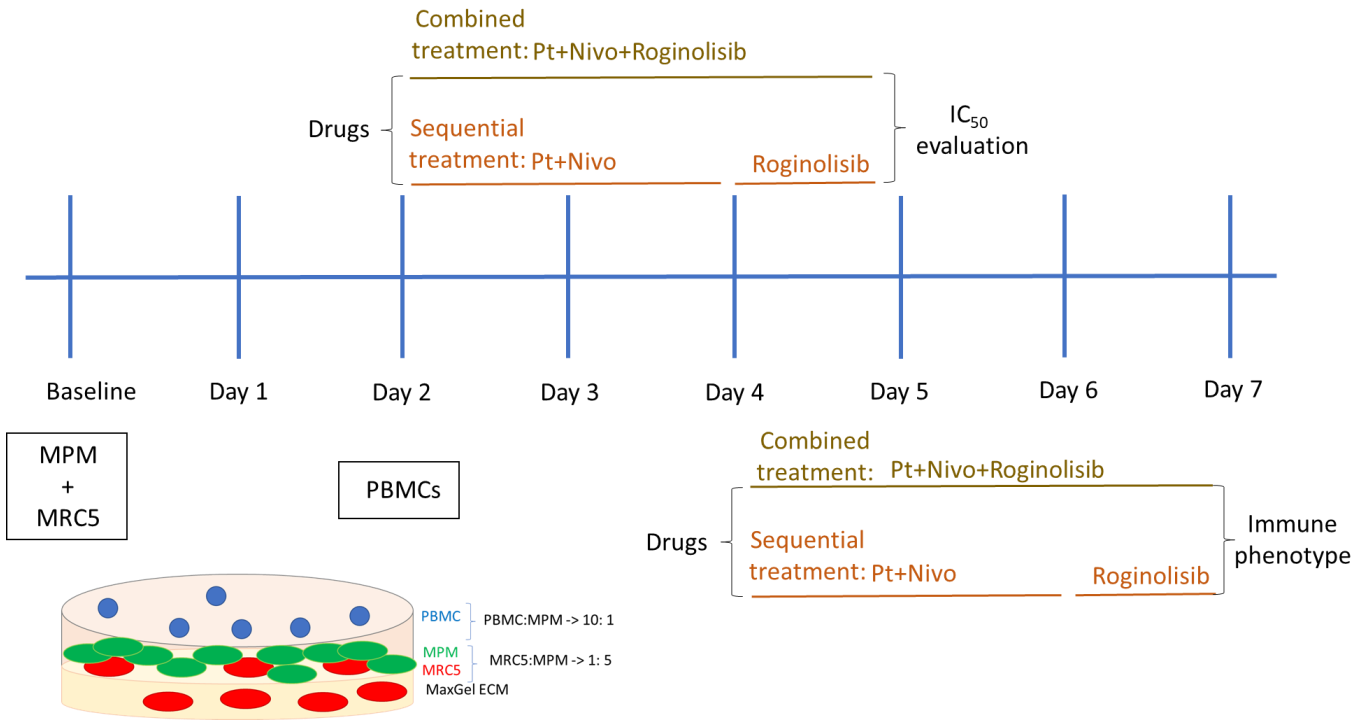

Supplemental Figure 1. Treatment Design to Evaluate Immune Marker Regulation with roginolisib, Nivolumab and Cisplatin of patient-derived malignant pleural mesothelioma (MPM) cells matched with autologous peripheral blood mononuclear cells (PBMCs). Using fibroblast cell line MRC5 as feeder cells, MPM cells are cultured on a MaxGel ECM (extracellular matrix) plate (initial ratio at 1:5). After 2 days, PBMCs are added (ratio of MPM to PBMC 1:10), and the co-culturd cells are treated with (roginolisib, alone or combined with platinum (Pt) and nivolumab (Nivo). At Day 5 IC50 evaluation is performed, and at Day 7 the immune cells are being evaluated using flow cytometry.

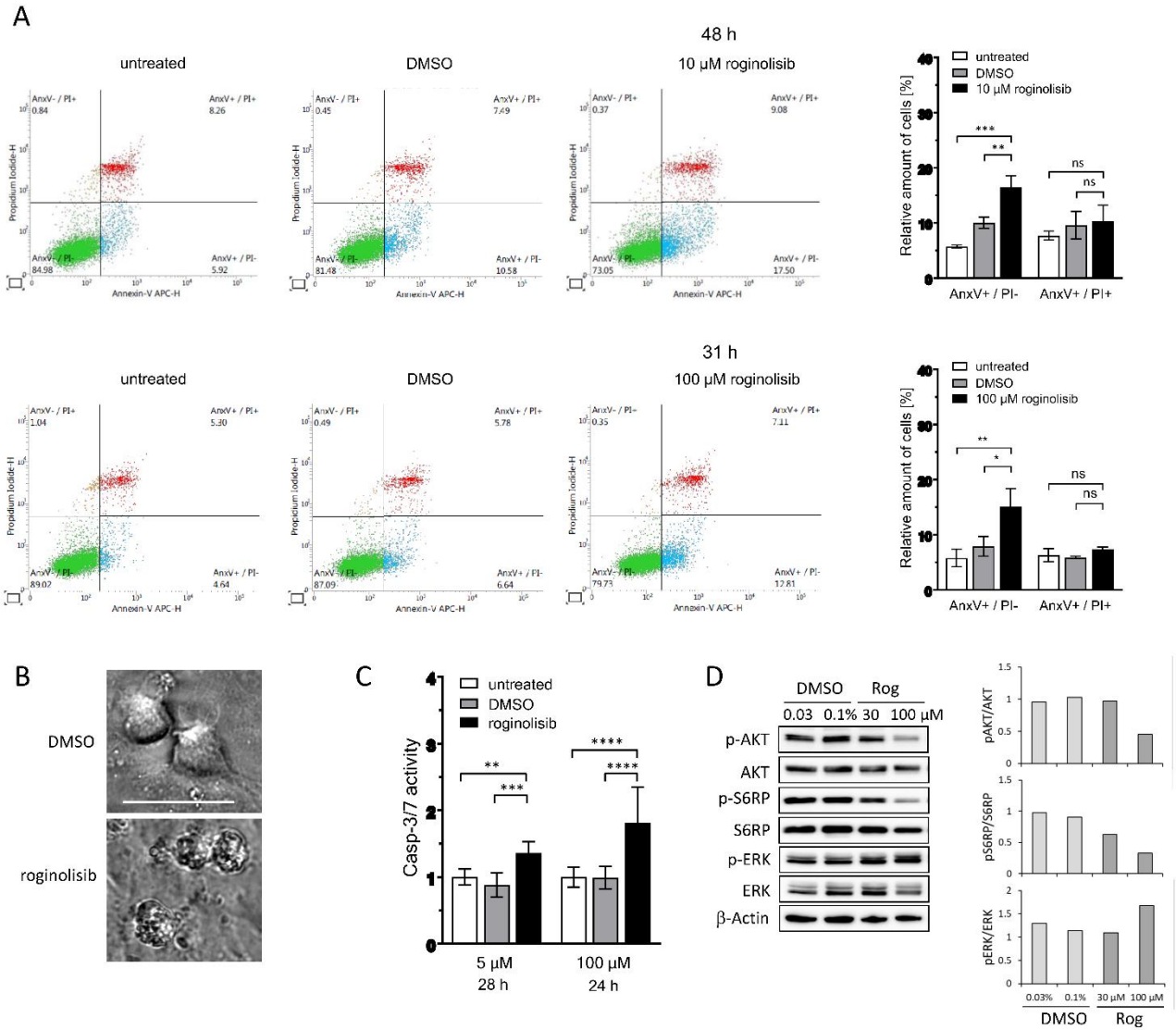
A
48 h
untreated
DMSO
10 µM roginolisib
AnxV- / PI+
AnxV+ / PI+
AnxV- / PI-
AnxV+ / PI-
0.84
8.26
84.98
5.92
0.45
7.49
81.48
10.58
0.37
9.08
73.05
17.50
Propidium Iodide-H
Annexin-V APC-H
untreated
DMSO
10 µM roginolisib
Relative amount of cells [%]
***
**
ns
ns
AnxV+ / PI-
AnxV+ / PI+
31 h
untreated
DMSO
100 µM roginolisib
1.04
5.30
89.02
4.64
0.49
5.78
87.09
6.64
0.35
7.11
79.73
12.81
untreated
DMSO
100 µM roginolisib
**
*
ns
ns
AnxV+ / PI-
AnxV+ / PI+
B
DMSO
roginolisib
C
untreated
DMSO
roginolisib
Casp-3/7 activity
**
***
****
****
5 µM
28 h
100 µM
24 h
D
DMSO
Rog
0.03
0.1%
30
100 µM
p-AKT
AKT
p-S6RP
S6RP
p-ERK
ERK
β-Actin
pAKT/AKT
pS6RP/S6RP
pERK/ERK
0.03%
0.1%
30 µM
100 µM
DMSO
Rog

Supplemental Figure 2. **Roginolisib induces apoptotic cell death in mesothelioma PXF1752 cells.** (A) Effects of roginolisib treatment (10 µM, 48 h; 100 µM, 31 h) on apoptosis induction in PXF1752 cells detected by flow cytometry using Annexin-V/PI staining, compared to DMSO (0.1%) and incubation with medium only (untreated cells). A significant increase in AnxV+/PI- cells is indicative of apoptotic cell death. Data points, mean of duplicate or triplicate samples, representative of independent duplicate experiments. 2way ANOVA test (Dunnett's multiple comparison); ***, p=0.0003; **, p=0.0032/0.0056; *, p=0.0111; ns, p>0.05. (B) Caspase-3/7 activity after roginolisib treatment (5 µM, 28 h; 100 µM, 24 h). Data points, mean ± SD of independent triplicate experiments. 2way ANOVA test (Dunnett's multiple comparison); ****, p<0.0001; ***, p=0.0001; **, p=0.0074. (C) Apoptotic membrane blebbing after treatment of PXF1752 cells with 100 µM roginolisib for 24 h, detected by phase-contrast microscopy. (D) Immunoblot analysis of PI3K/AKT pathway components p-AKT (S473) and p-RPS6 (S235/236), and p-ERK1/2 (T202/204) in response to increasing concentrations of roginolisib (Rog) in PXF1752 after 4 h of treatment. Bar graphs represent semi-quantitative analysis of phospho-protein expression relative to total protein, normalized to protein levels at 0 h.

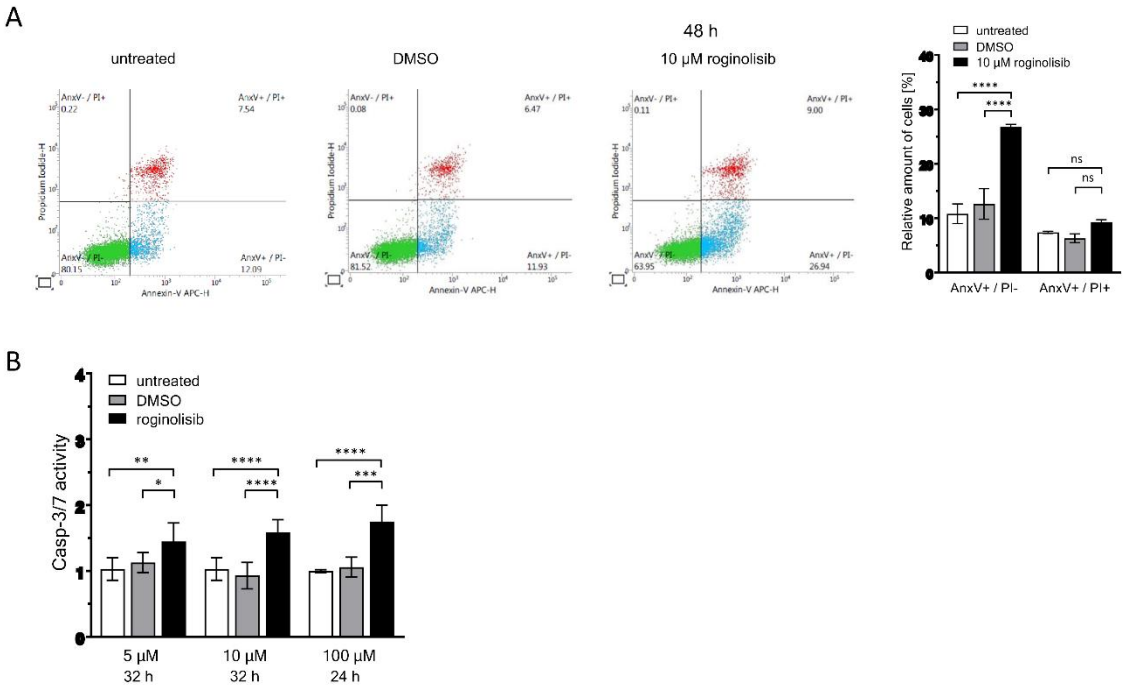

Supplemental Figure 3. **Roginolisib induces apoptotic cell death in mesothelioma PXF698 cells.** (A) Effects of roginolisib (10 µM) treatment for 48 h on apoptosis induction in PXF698 cells detected by flow cytometry using Annexin-V/PI staining, compared to DMSO (0.01%) and incubation with medium only (untreated cells). A significant increase in AnxV+/PI- cells is indicative of apoptotic cell death. Data points, mean of duplicate or triplicate samples, representative of independent duplicate experiments. 2way ANOVA test (Dunnett‘s multiple comparison); ****, $p<0.0001$; ns, $p>0.05$. (B) Caspase-3/7 activity after treatment (5 µM, 32 h; 10 µM, 32 h; 100 µM, 24 h). Data points, mean ± SD of at least two independent experiments. 2way ANOVA test (Dunnett‘s multiple comparison); ****, $p<0.0001$; ***, $p=0.0002$; **, $p=0.002$; *, $p=0.019$.

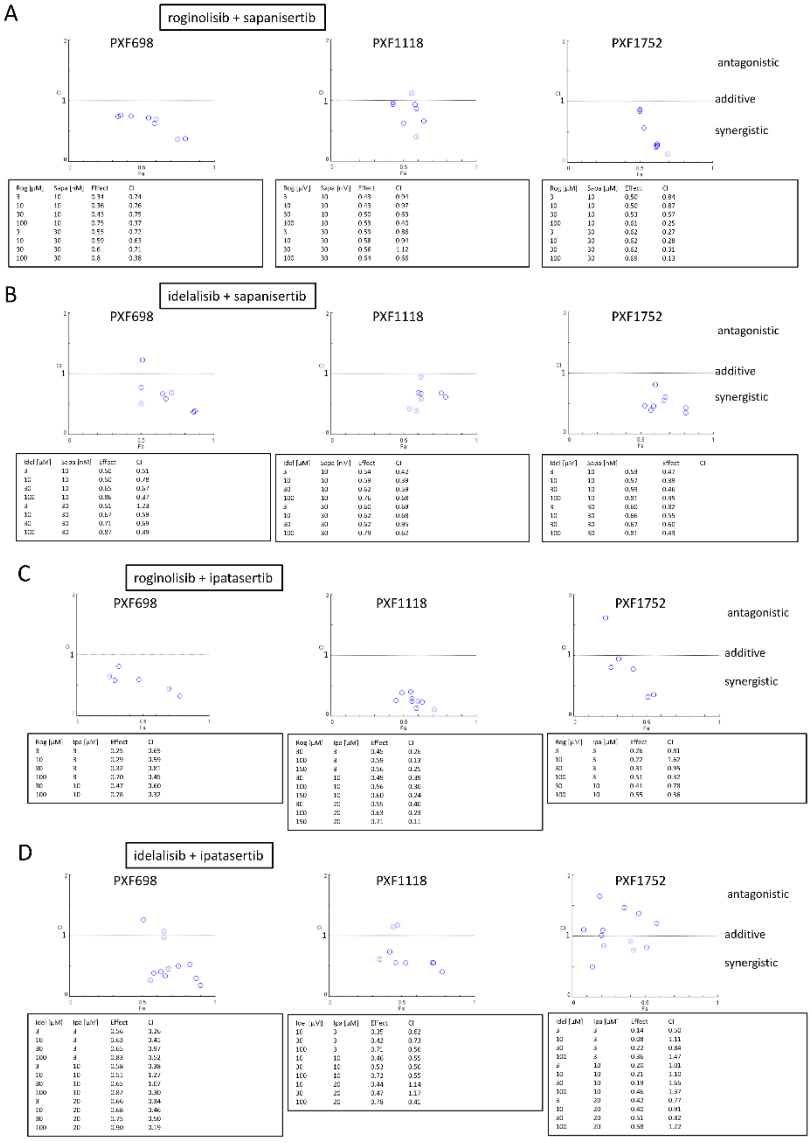
A
roginolisib + sapanisertib
PXF698
PXF1118
PXF1752
antagonistic
additive
synergistic
B
idelalisib + sapanisertib
PXF698
PXF1118
PXF1752
antagonistic
additive
synergistic
C
roginolisib + ipatasertib
PXF698
PXF1118
PXF1752
antagonistic
additive
synergistic
D
idelalisib + ipatasertib
PXF698
PXF1118
PXF1752
antagonistic
additive
synergistic

Supplemental Figure 4. **Simultaneous inhibition of PI3K-δ/mTOR and PI3K-δ/AKT.** Cell survival studies after treatment of MPM cell lines PXF698, PXF1118 and PXF1752 with (A) roginolisib/sapanisertib, (B) idelalisib/sapanisertib, (C) roginolisib/ipatasertib and (D) idelalisib/ipatasertib for 72 h. The CompuSyn software for evaluating drug combinations was used to generate a combination index (CI) of each combination listed in the associated tables [23]. CI < 1 synergistic, C = 1 additive, CI > 1 antagonistic. Effect, mean of five replicate samples, two independent experiments.

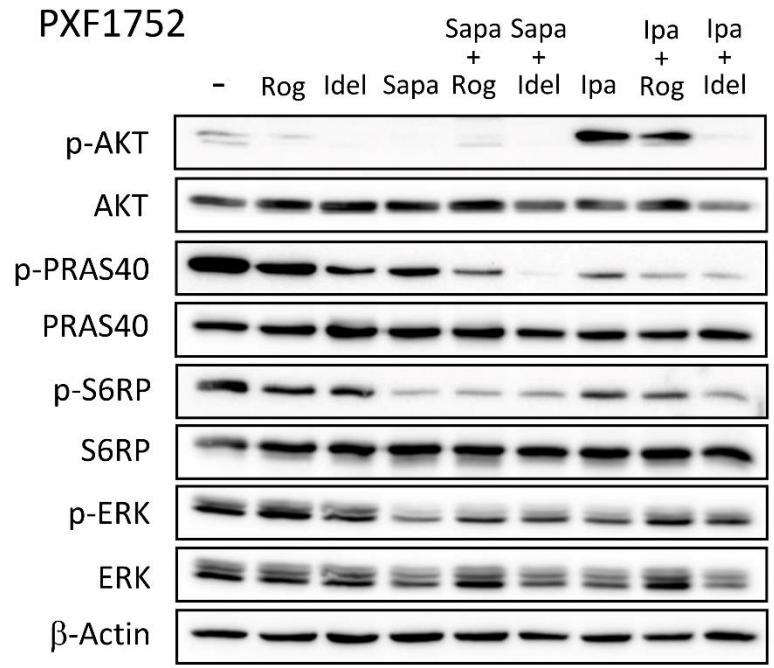

Supplemental Figure 5. **Molecular effects of simultaneous PI3K-δ/mTOR and PI3K-δ/AKT inhibition in mesothelioma PXF1752 cells.** Immunoblotting shows the levels of p-AKT (S473), p-PRAS40 p-PRAS40 (T246), p-RPS6 (S235/236) and p-ERK1/2 (T202/204) in PXF1752 cells treated with 100 μM roginolisib (Rog), 100 μM idelalisib (Idel), 30 nM sapanisertib (Sapa), 10 μM ipatasertib (Ipa), or their combinations as indicated for 4 h.

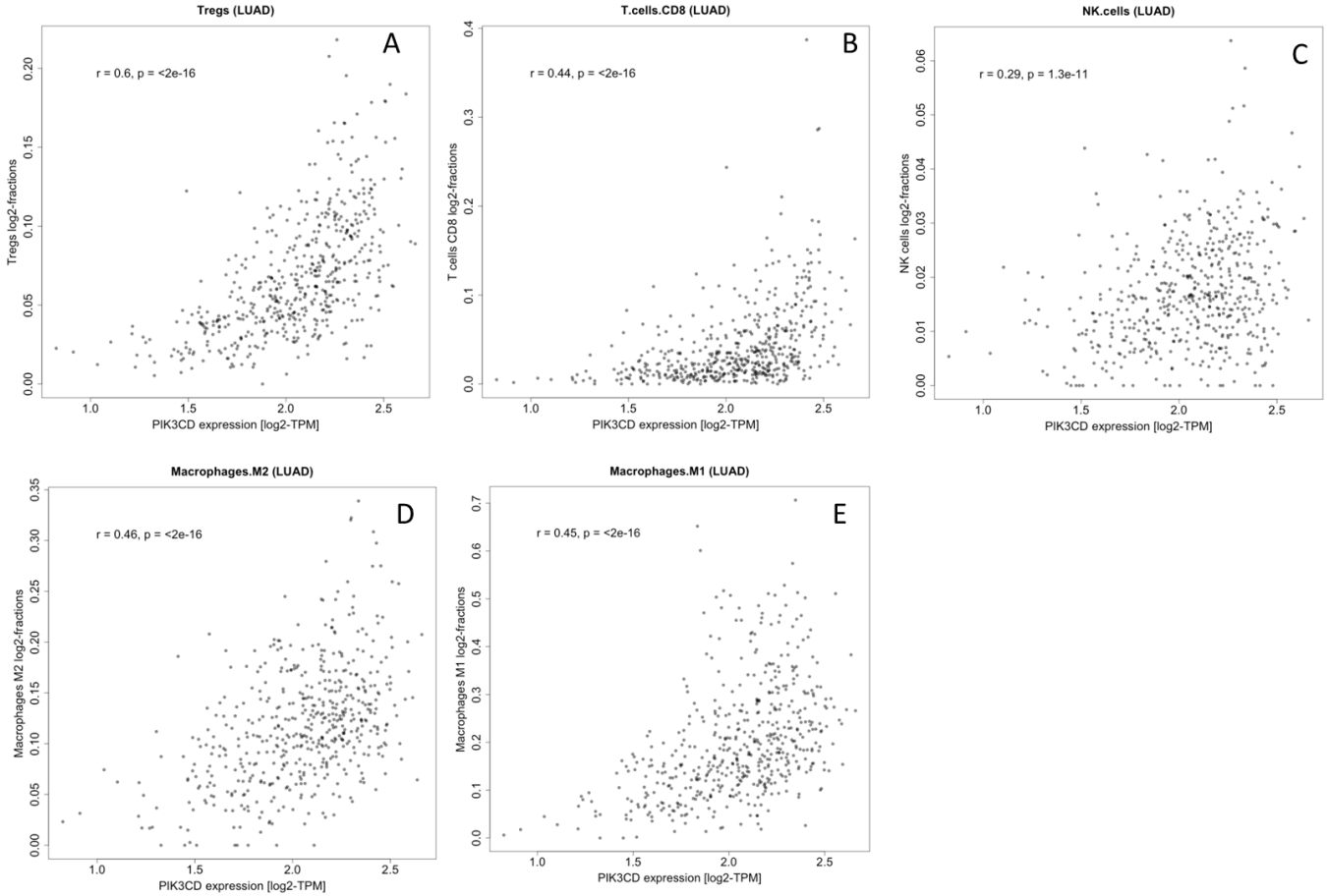

Supplemental Figure 6. Comparison of the PIK3CD gene expression with the abundance of immune cells in NSCLC (lung adenocarcinoma).

PIK3CD gene expression data from TCGA data sets (n=515 lung adenocarcinoma samples, LUAD) were plotted against an immune profile for Tregs (A), $CD8^+$ T-cells (B), Natural Killer (NK) cells (C), M2 macrophages (D) and M1 macrophages (E). r, correlation coefficient; p, p-value.

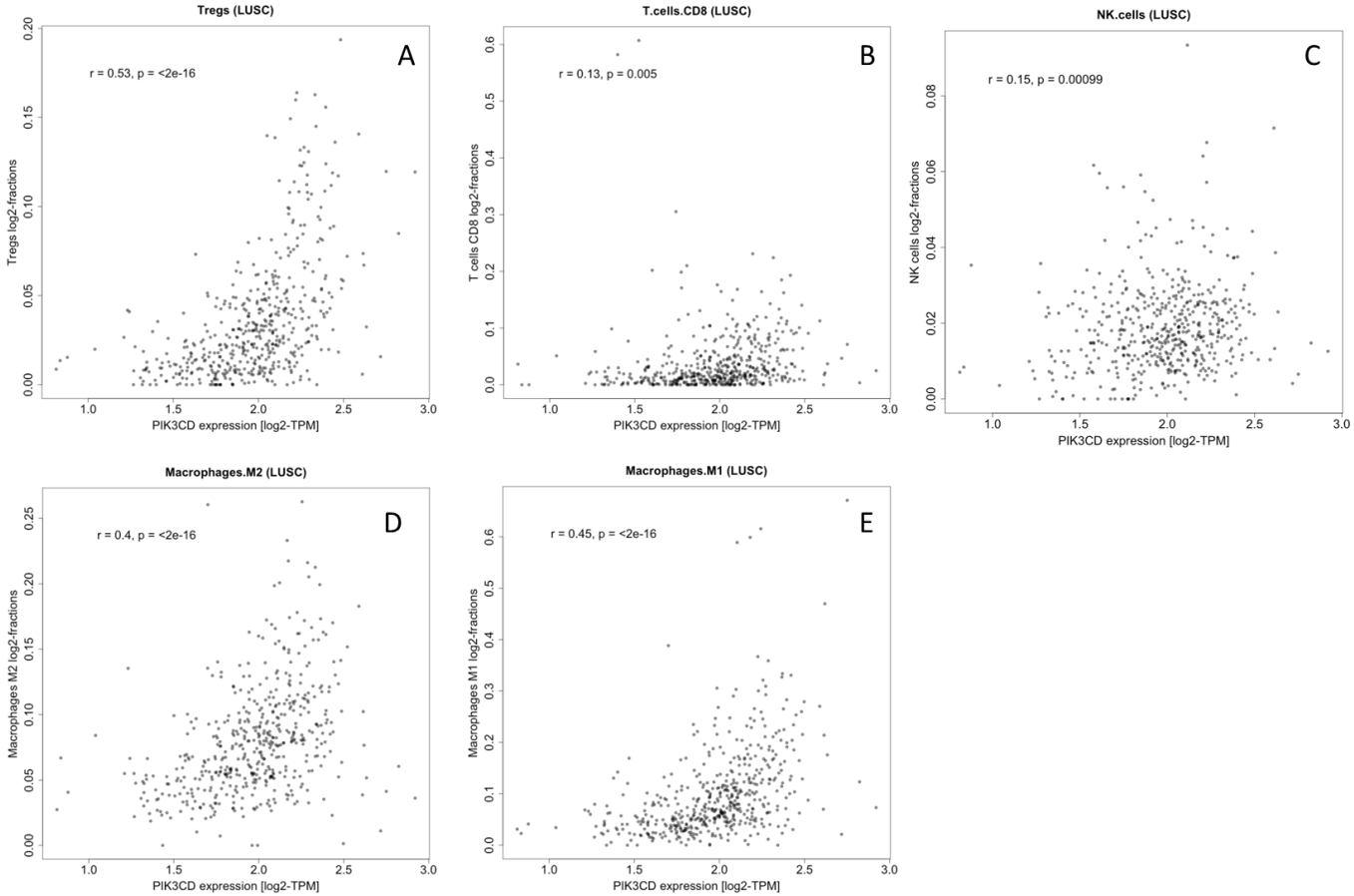

Supplemental Figure 7. Comparison of the PIK3CD gene expression with the abundance of immune cells in NSCLC (squamous cell carcinoma). PIK3CD gene expression data from TCGA data sets (n=501 lung squamous cell carcinoma samples, LUSC) were plotted against an immune profile for Tregs (A), $CD8^+$ T-cells (B), Natural Killer (NK) cells (C), M2 macrophages (D) and M1 macrophages (E). r, correlation coefficient; p, p-value.

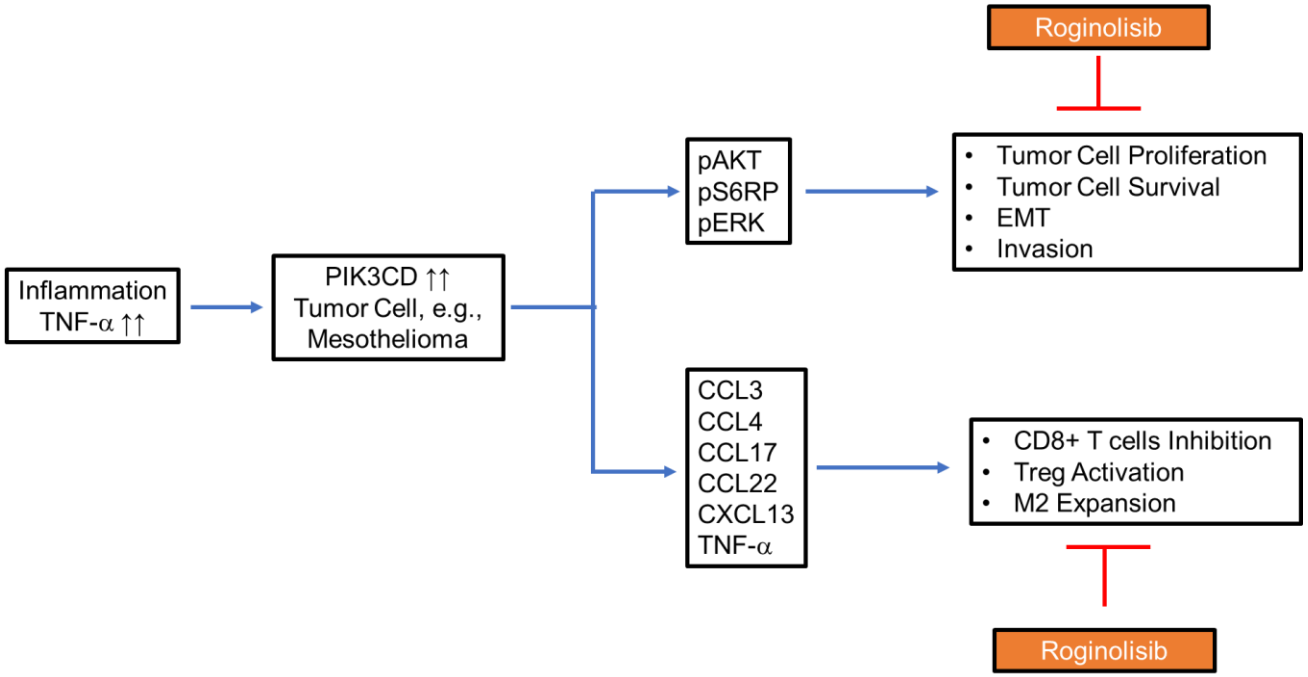

Supplemental Figure 8. Model of Antitumor Activity of Roginolisib Actiing on Tumor Cell-intrinsic and Tumor-Cell Extrinsic Mechanisms. Tumor cells express PIK3CD (e.g., induced by TNF-α), which in turn up-regulates canonical pathways in tumor cells via pAKT and pERK. This overall leads to an increase in tumor cell proliferation and survival, epithelial-mesenchymal transition (EMT) and invasion. At the same time, tumor cells secrete chemokines (e.g., C-C-motif ligand, CCL3, CCL4, CCL17, CCL22; C-X-C-motif ligand, CXCL13) and/or cytokines (e.g., Tumor necrosis factor alpha, TNF-α), which in turn are associated with tumor immune suppression as characterized by T regulatory (Treg) cell expansion/activation, M2 macrophage expansion and $CD8^+$ T cell inhibition. Roginolisib is designed to block both axes of this pathway as shown in this article.